Demonstration of Network Level Pavement Structural Evaluation with Traffic Speed Deflectometer: Final Report

Prepared for **the Federal Highway Administration**
Under Contract # DTFH61-11-D-00009-T-13008

By

Virginia Tech Transportation Institute

Subcontractor to

Engineering & Software Consultants, Inc.

May 2017

TABLE OF CONTENTS

<table>
<tr><td>Report No.:</td><td>Report Date:
May 2017</td><td>No. Pages:
35</td><td>Type Report:
Final Contract</td><td>Project No.:</td></tr>
<tr><td colspan="3" rowspan="2"></td><td>Period Covered:
October 2013 – February 2017</td><td>Contract No.:
DTFH61-11-D-00009-T-13008</td></tr>
<tr><td colspan="3">Title:
Demonstration of Network Level Structural Evaluation with Traffic Speed Deflectometer: Final Report</td><td rowspan="3">Key Words:
Traffic Speed Deflectometer, Deflection Testing, Non-Destructive Evaluation, Network-Level Decision Making, Structural Capacity Index</td></tr>
<tr><td colspan="3">Author(s): Samer Katicha*, Ph.D., Gerardo Flintsch*, Ph.D., P.E., Shivesh Shrestha*, and Senthilmurugan Thyagarajan**, Ph.D.</td></tr>
<tr><td colspan="3">Performing Organization Name and Address:
Virginia Tech Transportation Institute
3500 Transportation Research Plaza
Blacksburg, VA 24061</td></tr>
<tr><td colspan="5">Sponsoring Agencies' Name and Address:
Office of Infrastructure Research and Development
Federal Highway Administration
6300 Georgetown Pike
McLean, VA 22101-2296
and the State Department of Transportation of the States of California, Georgia, Idaho, Illinois, Nevada, New York, Pennsylvania, South Carolina and Virginia</td></tr>
<tr><td colspan="5">Supplementary Notes:
The Contracting Officer's Representative was Nadarajah Sivaneswaran, HRDI-20.
* affiliated with VTTI; ** affiliated with ESCINC</td></tr>
<tr><td colspan="5">Abstract:
The objective of this transportation pooled fund study was to carry out a field demonstration of the Traffic Speed Deflectometer (TSD) in the nine participating state highway agencies (SHAs) and present an approach of how the results of TSD testing could be implemented within a pavement management system (PMS). The testing was performed on a total of 5,928 miles (some repeated) during three time periods: November 2013, May to July 2014, and June to September 2015 and the results are summarized in this report. Specifically this report (1) describes the TSD and its measurement methods, (2) describes the collected data and the data processing performed (with details in the Appendix), (3) evaluates the short-term and long-term repeatability of the TSD, (4) presents a comparison between TSD and falling weight deflectometer (FWD) measurements, (5) presents a comparison between the data derived from TSD measurements and typical PMS data collected by state highway agencies, (6) shows how information obtained from the collected TSD data can be used to identify structurally strong and weak pavement sections, and (7) presents an approach that can be implemented by state highway agencies to incorporate indices derived from TSD data into their PMS decision-making process. Companion reports, documenting SHA-specific data analysis, findings, and recommendations have also been prepared and provided to each participating SHA.
The results of the testing showed good short-term and long-term repeatability of the TSD, as it was found that repeated measurements followed similar trends. However, there could still be improvements in TSD repeatability, especially in terms of temperature correction of TSD measurements and the TSD device calibration procedure in few sections. TSD measurements were also found to be comparable to FWD measurements in that measurements from both devices followed similar trends. Comparing TSD measurements with PMS surface condition data found, as suspected, that the TSD provided valuable information about the structural condition of the tested pavement sections that cannot be derived from the already available pavement surface condition as part of an agency's PMS. The TSD was found to be capable of differentiating between relatively structurally strong and weak sections and provide more detailed assessment when used in conjunction with SHA's PMS data. An example of how TSD information can be used to refine the triggered treatment category as part of a network-level PMS analysis is presented for a roughly 75-mile section of I-81 south in Virginia.</td></tr>
</table>

FIELD DEMONSTRATION OF THE TRAFFIC SPEED DEFLECTOMETER: FINAL REPORT

Samer Katicha[1], Gerardo Flintsch[1], Shivesh Shrestha[1], and Senthilmurugan Thyagarajan[2]

INTRODUCTION

This report summarizes the results from the Traffic Speed Deflectometer (TSD) demonstration transportation pooled fund project performed with the participation of nine state highway agencies (SHAs): Caltrans, Georgia Department of Transportation (DOT), Idaho Transportation Department, Illinois DOT, Nevada DOT, New York DOT, Pennsylvania DOT, South Carolina DOT, and Virginia DOT. There are two main objectives and three secondary objectives to the project. The two main objectives are:

1. Develop a framework that state highway agencies can adopt to obtain a structural classification of the road network in terms of good, fair, and poor condition. The classification is based on structural indices and threshold values for those indices. Threshold values could be based on a mechanistic-empirical approach (e.g., predicting remaining fatigue life) or on the distribution of index values (i.e., based on percentiles of the data; e.g., 25th and 95th percentiles of the selected index could be chosen to differentiate between good and fair, and between fair and poor). The two main indices presented in this report are the Structural Curvature Index 300 (SCI300) and Deflection Slope Index (DSI). Some example sections for which layer thicknesses were available were also used to show that the effective structural number (SN_{eff}) can be calculated from TSD measurements.
2. Demonstrate how structural information obtained from the TSD can be incorporated into a SHA's pavement management system (PMS). An example using a simplification of Virginia's approach is presented. The example uses a 74.1-mile section of I-81 south to determine which treatment category would be triggered without and with consideration of the structural condition.

The three secondary objectives focus on the evaluation of the quality of the measurements collected by the TSD and whether TSD measurements provide information that cannot be implied from the pavement surface condition data that are already being collected by most state highway agencies. These three secondary objectives are:

1. Short-term and long-term repeatability of TSD measurements. Short-term repeatability is evaluated with measurements performed on the same section during the same day or within a few days (generally a day or two). Long-term repeatability is evaluated with measurements performed on the same section at about a one-year interval. The focus in this project is network-level structural evaluation, and therefore the repeatability was

[1] Virginia Tech Transportation Institute
[2] Engineering & Software Consultants, Inc.

evaluated based on whether the trends of two repeated measurements were similar. The conditions (especially temperature) during repeated tests could be very different (although an experimental temperature correction approach is applied to the measurements), and therefore the focus is not on the actual magnitudes of the measurements but rather on how they vary along the tested sections. Note that previous studies have performed detailed evaluation of the repeatability of the TSD under more controlled testing conditions (e.g., Rada et al., 2016; Flintsch et al. 2013).

2. Comparison of TSD measurements with falling weight deflectometer (FWD) measurements. This evaluation was to assess whether the measurements from the two devices followed similar trends and whether the ranking of pavement sections (from weakest to strongest) based on TSD measurements is compatible with ranking based on FWD measurements.
3. Comparison of TSD measurements with PMS pavement condition data. The value of the TSD is its ability to collect information about the pavement (structural) condition that is not already reliably or adequately captured by other parameters currently collected and stored in a PMS. This comparison is made with pavement condition indices used by SHAs (namely Virginia, Pennsylvania, and Illinois), as well as fatigue cracking data (from Virginia), which is a load-related pavement distress.

OVERVIEW OF THE TSD

The TSD, shown in Figure 1, is an articulated truck with a rear-axle load that can be varied from 58.7 to 127.6 kN (13,196 to 28,686 lbf) by using sealed lead loads. The TSD has a number of Doppler lasers mounted on a servo-hydraulic beam to measure the deflection velocity of a loaded pavement. The TSD evaluated in this study used seven Doppler lasers. Six Doppler lasers were positioned to measure deflection velocity at 100, 200, 300, 600, 900, and 1,500 mm (3.9, 7.9, 11.8, 23.6, and 59 inches) in front of the loading axle. The seventh sensor was positioned 3,500 mm (11.5 ft) in front of the rear axle, largely outside the deflection bowl, to act as a reference laser. The beam on which the lasers are mounted moves up and down in opposition to the movement of the trailer in order to keep the lasers at a constant height from the pavement's surface. To prevent thermal distortion of the steel measurement beam, a climate control system maintains the trailer temperature at a constant 20°C (68°F). Data are recorded at a survey speed of up to 96 km/h (60 mph) at a rate of 1000 Hz.

Figure 1. TSD used during testing (left) and computer-generated schematic (right) (Krarup, 2012).

Measurement Technology

The TSD uses Doppler lasers mounted at a small angle to the vertical to measure the overall velocity that comprises the following components: (1) vertical pavement deflection velocity, (2) horizontal vehicle velocity, and (3) vertical and horizontal vehicle suspension velocity. Due to its location midway between the loaded trailer axle and the rear axle of the tractor unit, the pavement under the reference laser is expected to be outside the zone of load influence (undeformed). Its response is therefore used to remove the unwanted vertical and horizontal vehicle suspension velocity from the six measurement lasers. The horizontal velocity is also measured independently and used to determine the horizontal component of the velocity measured by the Doppler lasers. To remove the effect of vehicle speed, the deflection velocity is divided by the instantaneous vehicle speed to give a measurement of deflection slope, as illustrated in Figure 2. The deflection slope is calculated as follows:

$$S = \frac{V_v}{V_h} \tag{1}$$

where S is the deflection slope, V_v is the vertical pavement deflection velocity, and V_h is the vehicle horizontal velocity. Typically, deflection velocity is measured in mm/s and vehicle speed is measured in m/s; therefore, the deflection slope measurements are output in units of mm/m and generally averaged and reported at 10-m (33-ft) intervals. At a speed of 80 km/h (50 mph) and a data collection frequency of 1000 Hz, this corresponds to an average of 450 individual measurements over the 10-m section.

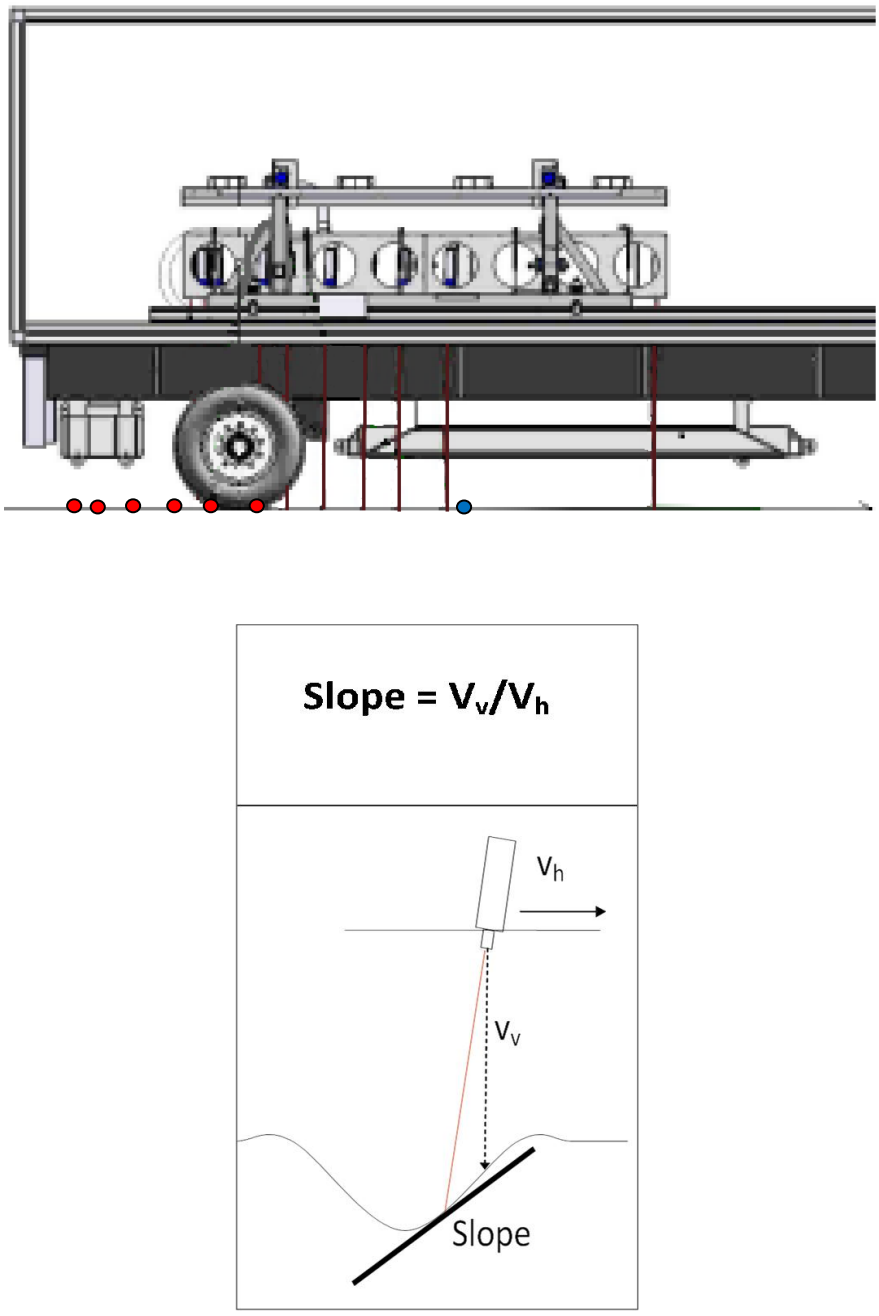

Figure 2. Measurement principle of the TSD (Krarup 2012 and Flintsch et al. 2013).

POOLED FUND STUDY PARTICIPANTS AND TOTAL MILES TESTED

Nine SHAs participated in the pooled fund study, with testing performed over three years: in November 2013, between May and July in 2014, and between June and September in 2015. Two data collection cycles were performed in all SHAs except Idaho and Virginia, which joined the pooled fund during the 2015 data collection cycle. In total, 5,928 lane miles (with some repeated testing) of testing were performed. The details for each state are shown in Table 1.

Table 1. Participating states and total tested lane miles.

Participating SHA	Testing month and year	Tested lane miles
Caltrans	June 2014 and August 2015	980
Georgia DOT	May 2014 and July 2015	646
Idaho Transportation Department	September 2015	1,040
Illinois DOT	June 2014 and September 2015	400
Nevada DOT	June 2014 and August 2015	352
New York DOT	November 2013 and July 2014	595
Pennsylvania DOT	July 2014 and June 2015	567
South Carolina DOT	May 2014 and July 2015	726
Virginia DOT	June 2015	622
Total		5,928

TSD Data Collection and Processing

Greenwood Engineering performed the data collection and provided the processed data in a series of Microsoft® Excel® files that included the data and roadway image files collected during testing. Details of the files provided in the external hard drive are given in Appendix A. Measured Global Positioning System (GPS) coordinates during testing were used to obtain the Google Map links to the location of the performed tests. Table 2 shows an example of generated links for the first round of testing performed in Illinois in 2014. Figure 3 shows an example of a link opened in a Web browser.

Table 2. Map link to location of performed tests in Illinois in 2014.

2014			
Test No.	File Name	Road Name	Map Link
1.	T7201406280001	I57 South 1	https://goo.gl/maps/n6xCNJT1hBF2
2.	T7201406280002	I57 North 1	https://goo.gl/maps/GQPU6pEsd8n
3.	T7201406280003	I57 South 2	https://goo.gl/maps/yF2tdFLbKFJ2
4.	T7201406280004	I57 North 2	https://goo.gl/maps/79mUCNkq2nr
5.	T7201406280005	I57 South 3	https://goo.gl/maps/bxkQf5jynEN2
6.	T7201406280006	I57 North 3	https://goo.gl/maps/CuU1a2bZu5s
7.	T7201406280019	3602 N Mattis Ave - 900 County Rd 3000 N	https://goo.gl/maps/mop8QzUAWz72
8.	T7201406300001	I57 South – I74 East	https://goo.gl/maps/8x7anEQRdVD2
9.	T7201406300002	I74 West - I57 North	https://goo.gl/maps/RsNGhrQFfN22
10.	T7201406300003	I57 South 4	https://goo.gl/maps/61dwdSK96XT2
11.	T7201406300004	I72 West	https://goo.gl/maps/h7swrWc3ET82
12.	T7201406300005	SR29 East	https://goo.gl/maps/UmevQei4yYk
13.	T7201406300006	US51 North	https://goo.gl/maps/t1tGvDHatcA2

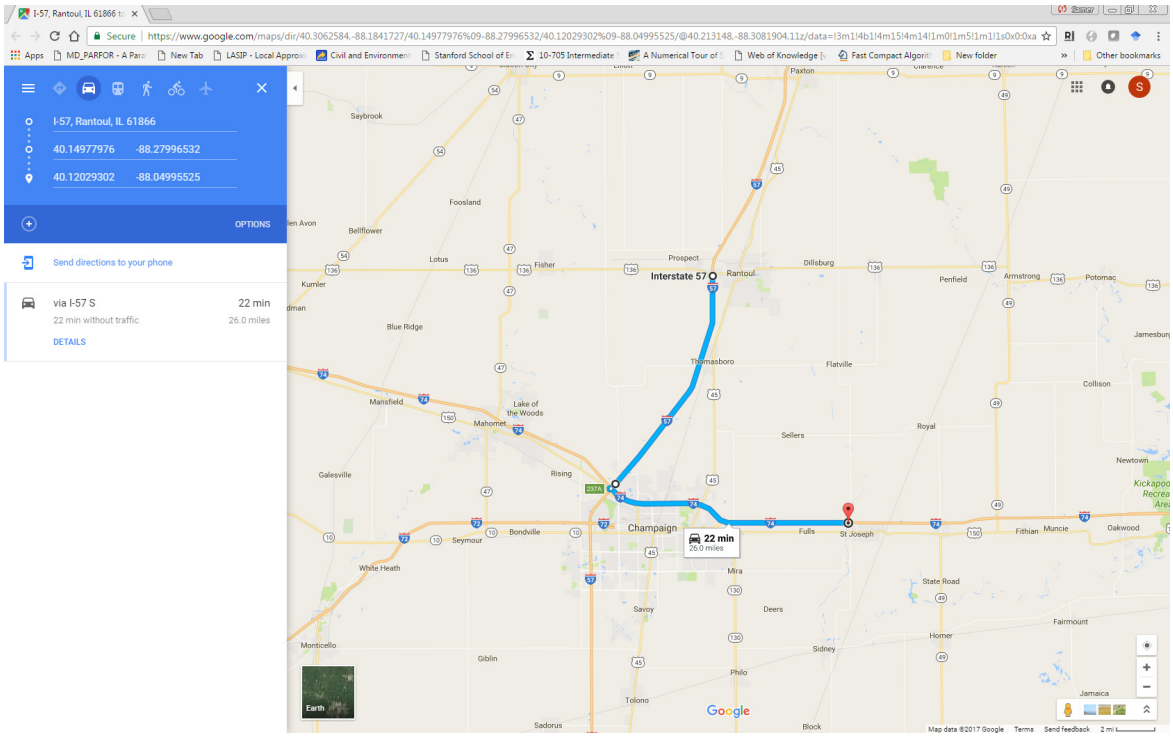

Figure 3. Google Maps© link showing test location on I-57 and I-74 for file "T7201406300001" in Table 2.

The calculated deflections provided by Greenwood Engineering were normalized with the measured dynamic load during testing and used to calculate the SCI300 and DSI as follows:

$$SCI300 = D0 - D300 \tag{2}$$

$$DSI = D100 - D300 \tag{3}$$

where D0 is the deflection at the point of load application (mid-point between the dual tires), and D100 and D300 are the deflections at 100 mm and 300 mm away from the point of load application.

The SCI300 and DSI were then corrected to a mid-depth reference temperature of 70°F using the procedure developed in Rada et al. (2016). The mid-depth temperature during testing was estimated using the BELLS3 equation (Lukanen et al. 2000) and the pavement surface temperature measured during testing. The overall procedure is outlined in the section "Temperature Correction Procedure." Finally, the temperature-corrected SCI300 (or DSI) was used to classify the pavement structural condition into the three categories of good, fair, and poor as outlined in the section "Determination of Default Thresholds for Pavement Structural Condition Classification." Figure 4 shows an example of calculated SCI300. The color-coded pavement structural condition was also plotted in Google Earth. Figure 5 shows the tested Nevada

network structural condition as an example. The detailed condition of a road near Carson City is shown in Figure 6.

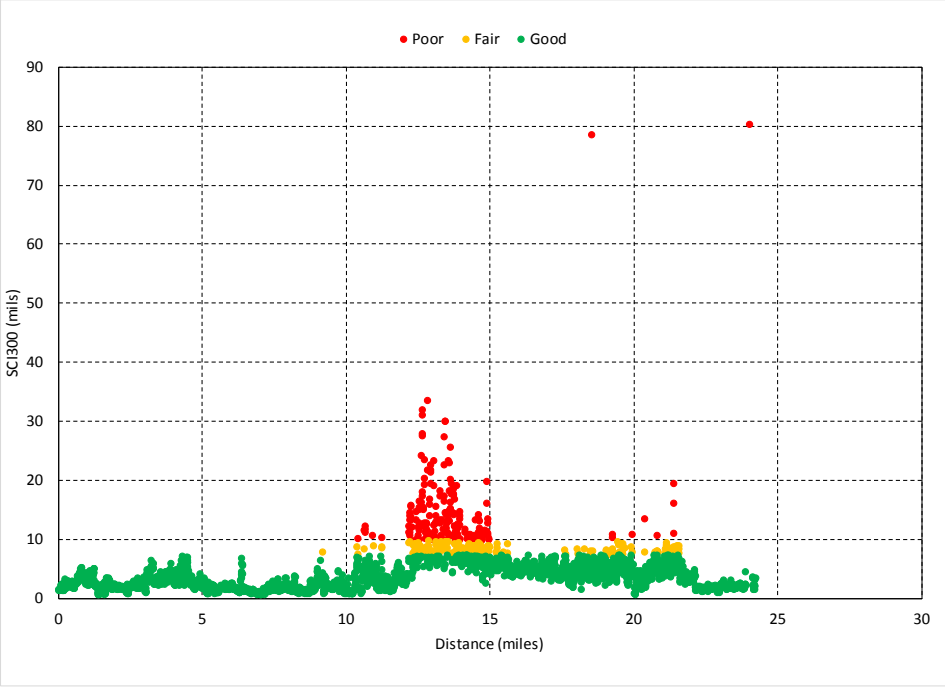

Figure 4. Example color-coded plot of structural condition SCI300 from the file "T720150100005."

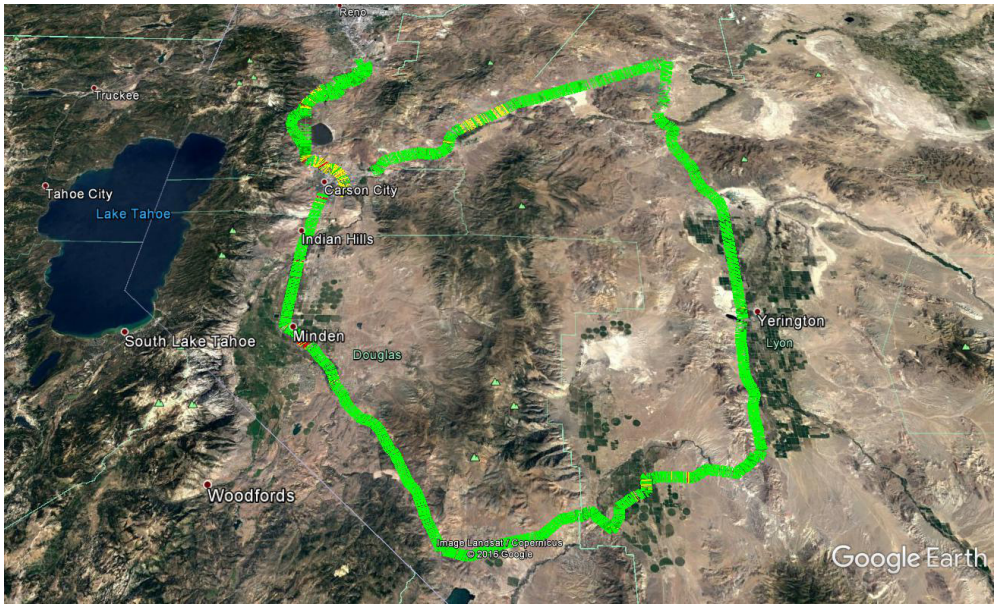

Figure 5. Google Earth color-coded pavement structural condition of tested pavements in Nevada with good (green), fair (yellow), and poor (red) ratings (© 2016 Google Image Landsat/Copernicus).

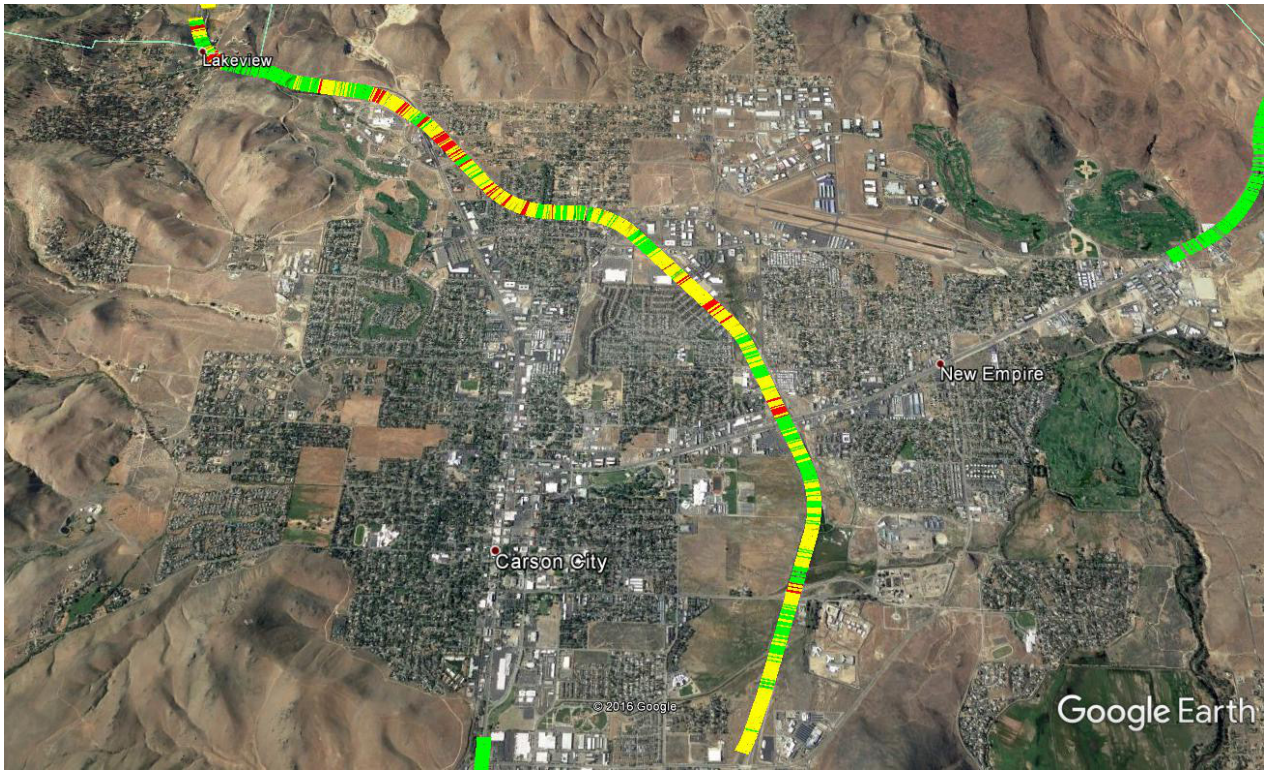

Figure 6. Detail from Figure 5 near Carson City, Nevada (© 2016 Google Image Landsat/Copernicus).

Calculation of Indices

The TSD measures the deflection slope of the deflection basin rather than pavement deflection. The deflection can be obtained from the deflection slope by integration as follows:

$$d(x) = \int_x^\infty s(y)dy \qquad (4)$$

where,

$s(y)$ = slope at distance y measured from the applied load;

$d(x)$ = deflection at distance x measured from the applied load.

Greenwood Engineering uses a parametrized model for the shape of the deflection slope developed by Pedersen et al. (2013) to obtain deflections from the deflection slope by optimizing the model parameters to fit the deflection slope data. The deflections computed from this model are reported in the data file (with extension .tsd.tsddefl.xls) and are used in this report. From the calculated deflections, the SCI300 and DSI were calculated. From the SCI300 and DSI, the tensile strain is calculated using Equation 5:

$$\varepsilon = a(DSI)^b \qquad \varepsilon = a'(SCI\,300)^{b'} \qquad (5)$$

The parameters *a*, *b*, *a'*, and *b'* are given in Table 3 and Table 4. These parameters depend on the thickness of the asphalt layer and were obtained by Rada et al. (2016).

Table 3. Relationship between DSI and maximum tensile strain at the bottom of the asphalt layer.

AC Layer Thickness	Parameter	
	a	*b*
3-4 inches	66.96	0.9351
4-5 inches	62.567	1.0174
5-6 inches	64.660	1.0379
6-7 inches	71.646	1.0005
7-8 inches	74.381	0.9757
8-9 inches	76.458	0.9427
9-10 inches	77.802	0.9107
10-11 inches	77.868	0.8674
11-12 inches	76.861	0.8395
12-13 inches	75.154	0.8149
13-14 inches	72.194	0.778
14-15 inches	70.196	0.7824
15-16 inches	66.402	0.7525
3-6 inches (Thin)	69.100	0.9348
6-9 inches (Medium)	75.100	0.9532
9-16 inches (Thick)	75.170	0.8579

Table 4. Relationship between SCI300 and maximum tensile strain at the bottom of the asphalt layer.

AC Layer Thickness	Parameter	
	a'	*b*'
3-4 inches	52.438	0.9620
4-5 inches	50.814	1.0200
5-6 inches	53.725	1.0240
6-7 inches	59.704	0.9870
7-8 inches	62.539	0.9520
8-9 inches	64.595	0.9120
9-10 inches	65.645	0.8820
10-11 inches	65.656	0.8373
11-12 inches	64.639	0.8103
12-13 inches	63.058	0.7895
13-14 inches	60.592	0.7479
14-15 inches	58.494	0.7594
15-16 inches	55.386	0.7285
3-6 inches (Thin)	57.818	0.9270
6-9 inches (Medium)	63.202	0.9350
9-16 inches (Thick)	62.538	0.8412

Calculation of Effective Structural Number (SN_{eff})

The SN_{eff} can be calculated from TSD measurements using the method of Rohde (1994) as follows:

1. Determine the structure index *SIP* of the pavement as follows:
   $$SIP = D_0 - D_{1.5Hp} \quad (6)$$
   where:
   D_0 = peak deflection under the 9,000-lb load
   $D_{1.5Hp}$ = deflection at lateral distance 1.5 times the pavement depth
   Hp = pavement depth – thickness of all layers above the subgrade
2. Determine the existing pavement SN_{eff} as:
   $$SN_{eff} = k_1 SIP^{k_2} H_p^{k_3} \quad (7)$$
   where for asphalt pavements, $k_1 = 0.4728$, $k_2 = -0.4810$, and $k_3 = 0.7581$. D_0 used in the calculation was corrected to a reference temperature of 68°F using the procedure described in Lukanen et al. (2000). $D_{1.5Hp}$ was assumed to be farther enough to be affected by temperature and consequently not temperature corrected.

Temperature-Correction Procedure

The temperature-correction procedure used was developed by Rada et al. (2016). The procedure corrects for the strain at the bottom of the asphalt layer, calculated using Equation 5, based on the change of the asphalt mix dynamic modulus as a function of temperature and the relationships between dynamic modulus and strain. After the temperature-corrected strain is obtained, the temperature-corrected indices (SCI300 and DSI) were obtained with the inverse of Equation 5. The steps for this procedure (from Rada et al. 2016) are as follows:

1. Compute the asphalt layer dynamic modulus at the test temperature, E_f, based on the calculated strain (from DSI or SCI300 using Equation 5) using the following equation:
   $$E_f = c \times \varepsilon^d \quad (8)$$
   where c and d are model parameters that depend on the asphalt layer thickness. When the thickness is not known, default values are provided.
2. Compute a temperature-correction factor, T_c, for the dynamic modulus as follows:
   $$T_c = 19.791\left(e^{-0.043T_r} - e^{-0.043T_f}\right) \quad (9)$$
   where T_r is the reference temperature (typically 70°F) and T_f is the asphalt temperature during the test.
3. Compute the dynamic modulus, E_r, at the selected reference temperature as follows:
   $$E_r = \frac{E_f}{1 - T_c} \quad (10)$$
4. Compute the strain, ε_r, at the selected reference temperature by rearranging Equation 6 as follows:
   $$\varepsilon_r = \left(\frac{E_f}{c}\right)^{\frac{1}{d}} \quad (11)$$
5. Calculate the temperature-corrected TSD index using the inverse of Equation 5.

The asphalt temperature T_f is taken as the mid-depth temperature and calculated from the measured surface temperature using the BELLS3 equation (Lukanen et al. 2000):

$$\begin{aligned} T_f &= 0.95 + 0.892 \times IR \\ &\quad + \left[\log(d) - 1.25\right] \times \left[-0.448 \times IR + 0.621 \times (1\text{day}) + 1.83 \times \sin(\text{hr}18 - 15)\right] \\ &\quad + 0.042 \times IR \times \sin(\text{hr}18 - 13.5) \end{aligned} \quad (12)$$

where:

T_f = pavement temperature at mid-depth d, °C
IR = pavement surface temperature, °C
log = base 10 logarithm
d = mid-depth of the AC layer, mm

1day = average air temperature the day before testing, °C
sin = sine function on an 18-hr clock system, with 2π radians equal to one 18-hr cycle
hr18 = time of day, in a 24-hr clock system, but calculated using an 18-hr asphalt concrete (AC) temperature rise-and-fall time cycle

Greenwood Engineering reported GPS location and time at each interval (10 m) in the file ending with ".gpsimp.xls." Note that GPS time is presented in Coordinated Universal Time (UTC). Pavement surface temperatures are also reported along with deflections in the file ending with "tsd.tsd.xls." The previous day's average air temperature was obtained at the closest weather station from the National Center for Environmental Information weather site, https://gis.ncdc.noaa.gov, and used in Bells equation to calculate mid-depth temperature. The computed mid-depth temperature was used with the temperature-correction procedure described earlier. The following points should be noted when the results from temperature correction and repeatability analysis are evaluated:

- The temperature-correction model should be considered as an intermediate solution until an accurate procedure is develop.
- Pavement layer details were not readily available for all the tested sections and therefore, for the purpose of temperature corrections, all sections were assumed to be flexible pavements. Consequently, the temperature corrected SCI300 should only be used for those pavement sections that State DOT knows to be flexible pavements. For sections that are not flexible pavements, it is recommended to use the uncorrected SCI300 or other indices presented.
- AC layer thicknesses were obtained from the respective SHAs' PMSs or, when these were not available, assumed based on the road category (presented later in Table 5).
- Maintenance and rehabilitation (M&R) activities, if any, applied between the time of initial and repeat data collection were not considered in the repeatability analysis.

Determination of Default Thresholds for Pavement Structural Condition Classification

A methodology based on the number of remaining Equivalent Single Axle Loads (ESALs) was used to arrive at a preliminary estimate for the threshold between good/fair and fair/poor segments. The remaining ESAL thresholds used in the report are only for illustrative purposes and it is expected that they will be revised based on the experience gained from TSD implementation efforts by individual SHAs.

Thresholds were obtained for three road categories—interstate, primary, and secondary roads—based on asphalt layer thickness as shown in Table 5. The thresholds given in Table 5 are based on a large database of simulated pavement sections by Rada et al. (2016). The responses from

these simulated pavements were used to determine the number of load repetitions to failure, N_f, computed using the Asphalt Institute equation (Asphalt Institute, 1982)

$$N_f = C \times 0.00432 \left(\frac{1}{\varepsilon_t}\right)^{3.291} \left(\frac{1}{E}\right)^{0.854} \quad (12)$$

where C is the calibration coefficient, ε_t is the tensile strain at the bottom of the asphalt layer (load corresponding to 9,000 lbf loaded dual-tire configuration with 13.5-inch tire spacing and 116 psi tire pressure), and E is the stiffness of asphalt mixture (psi). The value of C was set to 13.3 for interstate and primary roads and 18.4 for secondary roads corresponding to the failure criteria of 10% and 45% of wheel-path cracking, respectively (Finn et al., 1977). To convert remaining ESALs to remaining life, the following default levels of annual ESAL traffic were considered for the three road categories:

- Interstate: 1.4 million ESAL – equivalent to about 6,500 Annual Daily Truck Traffic (ADTT) (or 2,000 singles, 4,000 doubles, and 500 trains or triples)
- Primary: 0.2 million ESAL – equivalent to about 950 ADTT (or 700 singles, 220 doubles, and 30 trains or triples)
- Secondary: 0.07 million ESAL – equivalent to about 375 ADTT (or 300 singles, 75 doubles).

Thresholds were set so that a pavement with 2 years or less of life remaining is considered "poor," between 2 and 5 years "fair," and 5 or more years "good." The two strain levels that separate good from fair and fair from poor can be obtained from Equation 12. These strains were then used to determine the appropriate SCI300 and DSI thresholds using Equation 5, which are given in Table 5.

Table 5. Thresholds for SCI300 (TSD) and DSI.

Road Category	AC layer thickness, inch	Annual Traffic, million ESAL	Threshold for Fatigue Cracking at Wheelpath, %	Threshold for Poor			Threshold for Fair		
				N_f, million ESAL	SCI300, mil	DSI, mil	N_f, million ESAL	SCI300, mil	DSI, mil
Interstate	> 9	1.4	10	2.8	3.7	3.0	7.0	2.7	2.2
Primary	6 - 9	0.2	10	0.4	6.2	5.2	1.0	4.9	4.0
Secondary	3 - 6	0.07	45	0.14	9.7	7.7	0.35	7.3	5.8

SHORT-TERM AND LONG-TERM REPEATABILITY OF THE TSD

Two examples of short-term repeatability and four examples of long-term repeatability are presented in this section. The reason more focus is placed on long-term repeatability is because comparatively it has been much less investigated than short-term repeatability. Figure 7 and Figure 8 show two examples of short-term SCI300 repeatability of tests (corrected to a reference

temperature of 70°F) performed in New York and Virginia, respectively. In both cases, the repeated runs followed similar trends. The tested section in Virginia being much longer, a smoothed SCI300 is also shown in the figure to better highlight the trends.

Figure 9, Figure 10, and Figure 11 provide examples of long-term repeatability of sections tested in Pennsylvania, Georgia, and Illinois, respectively. In all cases, the repeated SCI300 (corrected to a reference temperature of 70°F) followed similar trends, although Figure 10 shows a significant difference in the average measured SCI300 in Georgia, with 2014 collected measurements having higher SCI300.

In both cases the repeated SCI300 (corrected to a reference temperature of 70°F) follow similar trends although relatively less closely than in the case of short-term repeatability. This would be expected as, in general, more factors affect the long-term repeatability than that for the short-term. For example, the TSD had probably been recalibrated between the two repeated runs in the case of long term repeatability assessment and that could have contributed some of the differences. Similar to FWD and other pavement condition data collection devices, TSD sensors need to be periodically calibrated for accurate measurements. The calibration process is needed to derive a correction for the difference between the angles of the Doppler Lasers and the correction needs to be made to a high degree of precision. The calibration procedure ideally requires an approximately 1000 feet relatively straight, stiff and homogeneous pavement section. However, during the pooled fund testing, calibrations had to be conducted in the best available pavement sections within the vicinity of the testing locations and some of those sections may not have met all the required attributes of an ideal calibration section. In such cases, the correction may not have been precise and that could have contributed to some of the observed differences in the long-term repeatability assessment. For the short-term repeatability, the two runs were performed on consecutive days with the same calibration parameters. Also, any unexplained discrepancies in the long-term repeatability assessment that may be attributed to calibration shortcomings were isolated and affected only a few cases. Other factors are environmental conditions, especially temperature. For tests performed on consecutive days the environmental conditions are expected to be more similar than those performed a year apart.

In general, the long-term repeatability of the TSD was good, as is illustrated in Figure 12, which shows all repeated measurements in South Carolina. Note the difference observed in I85 North could be attributed to it being a composite pavement These represent measurements on different roads, with a cumulative total tested distance of more than 240 miles. Overall, the TSD measurements followed similar trends.

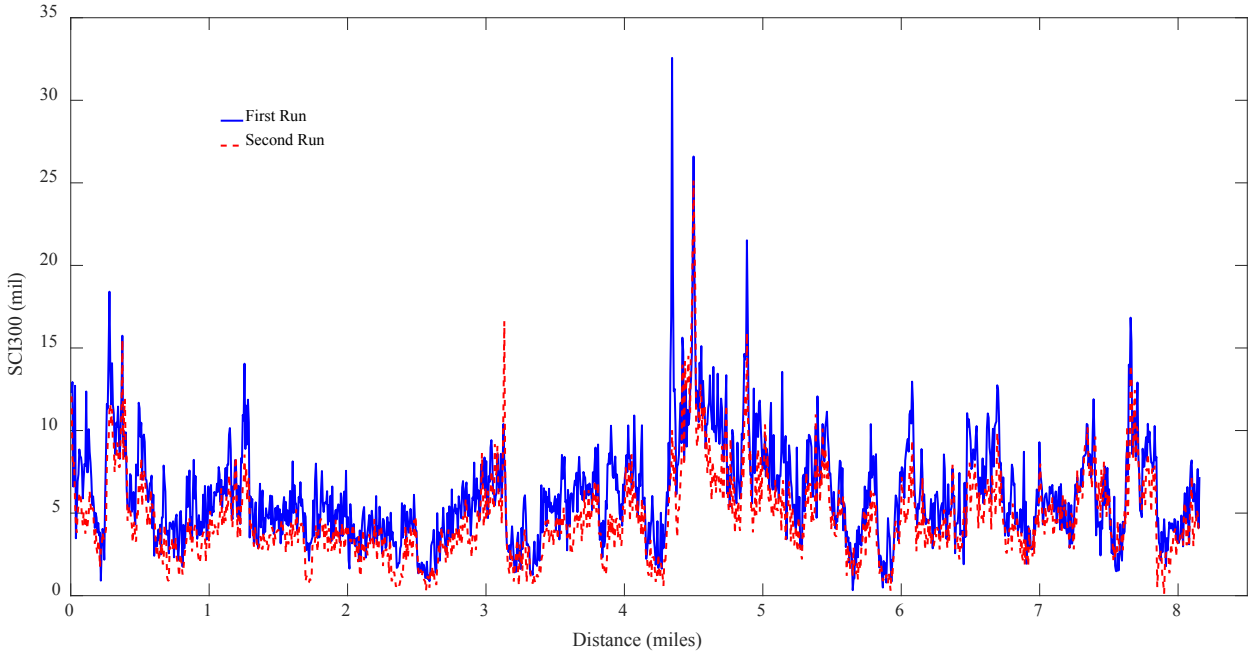

Figure 7. Short-term repeatability on SR 417 west in New York with tests performed on consecutive days in November 2013.

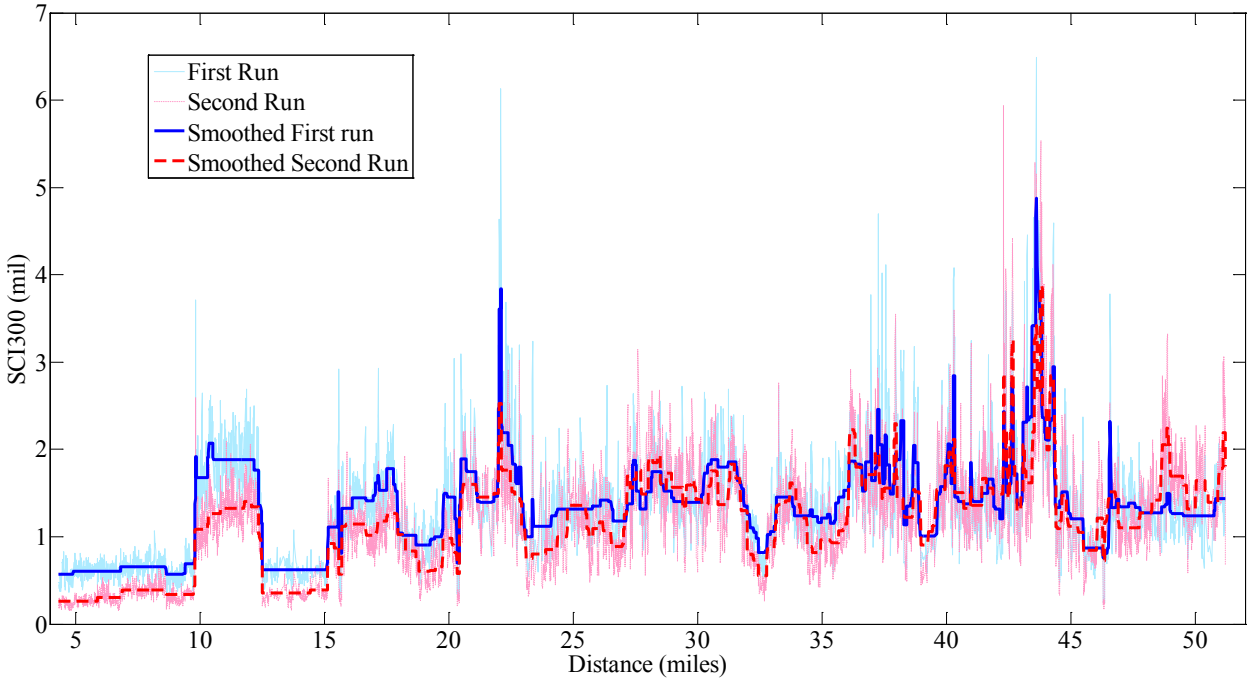

Figure 8. Short-term repeatability on US 29 south in Virginia performed on two consecutive days in June 2015.

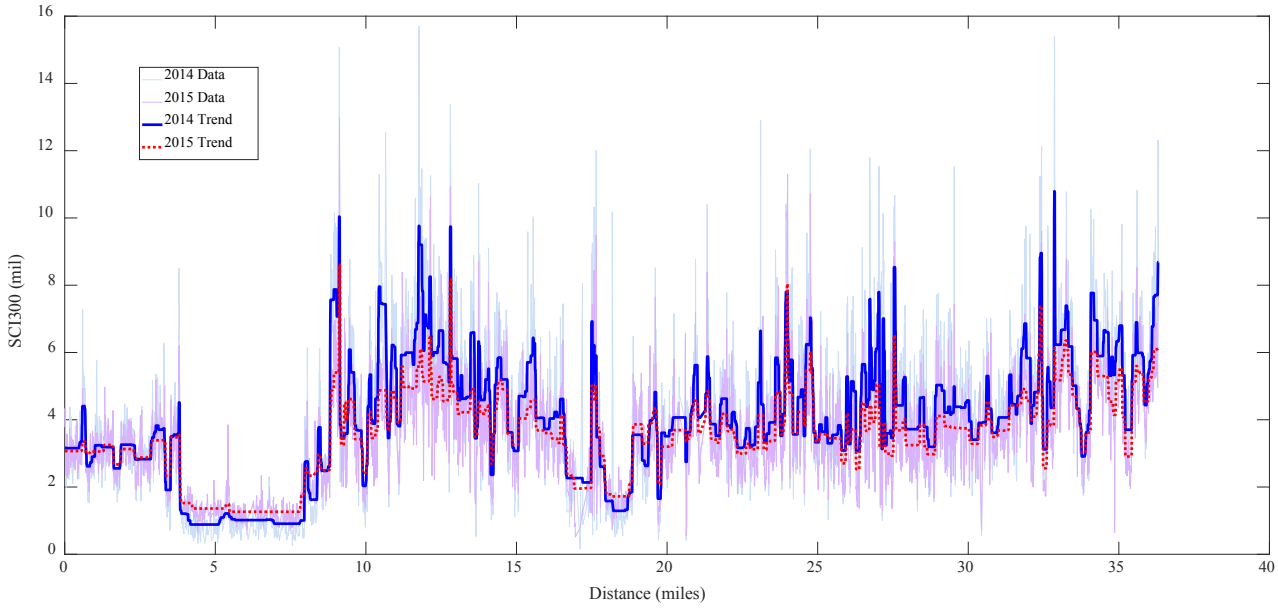

Figure 9. Long-term repeatability on Route 144 in Pennsylvania.

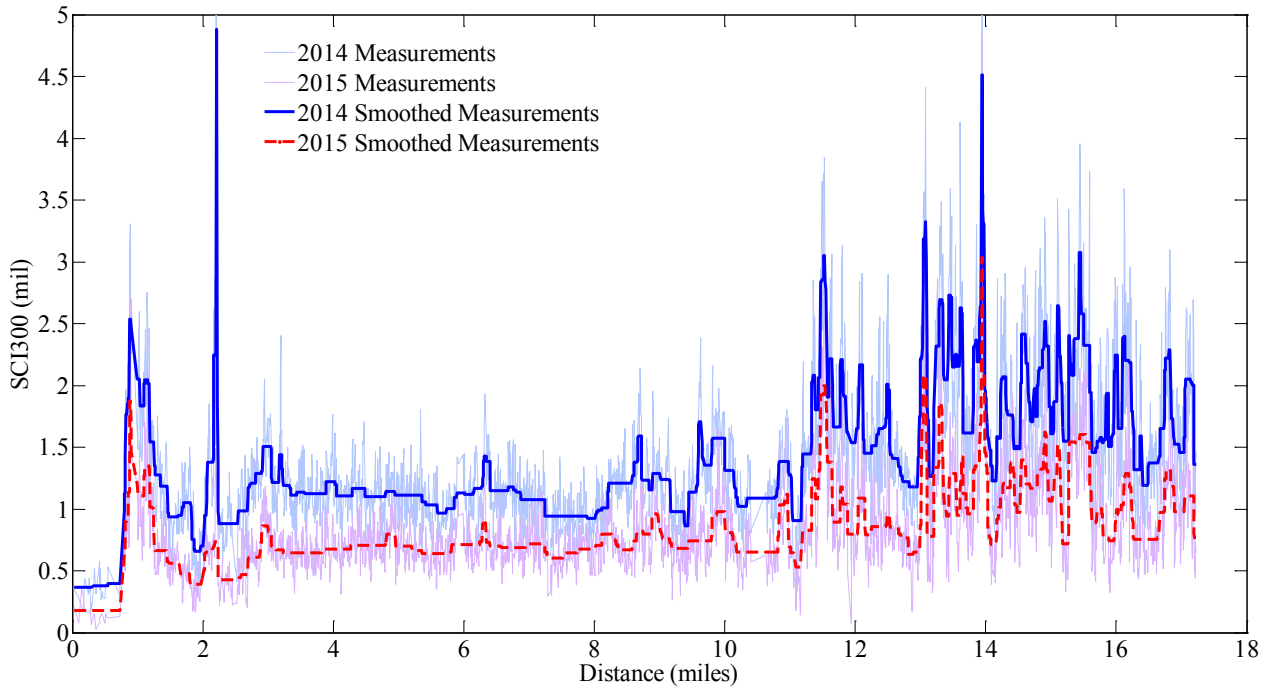

Figure 10. Long-term repeatability on Route 16 in Georgia.

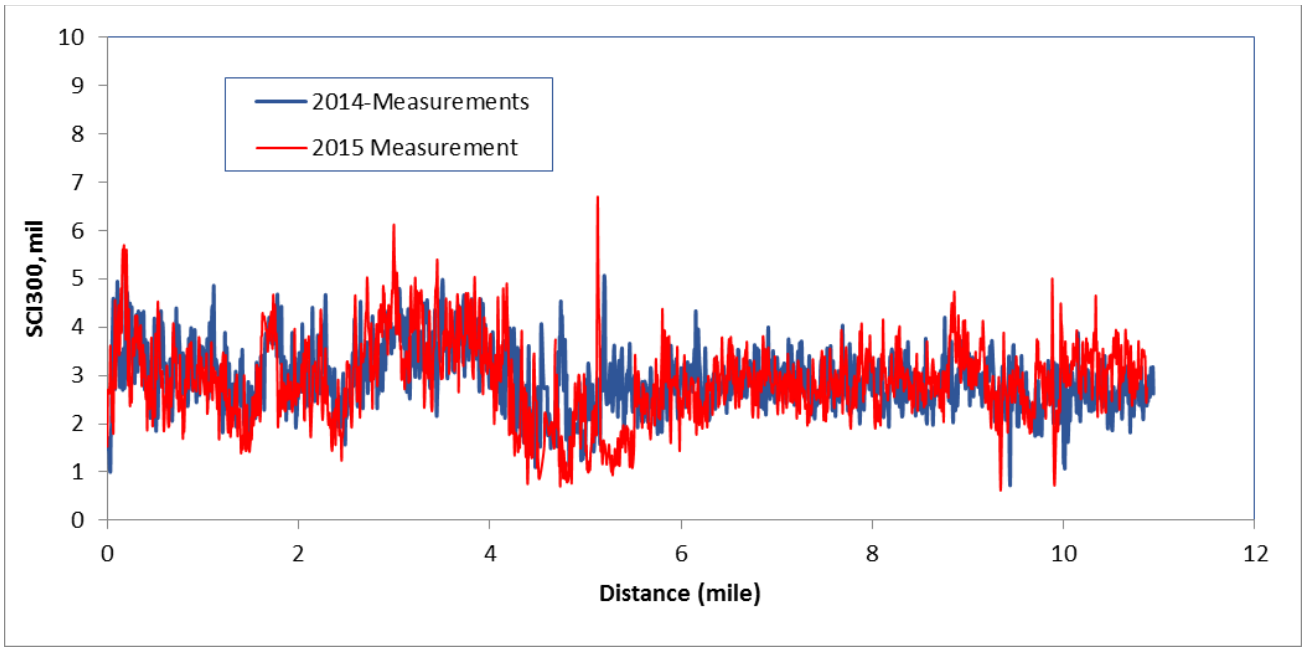

Figure 11. Long-term repeatability on a tested road in Illinois.

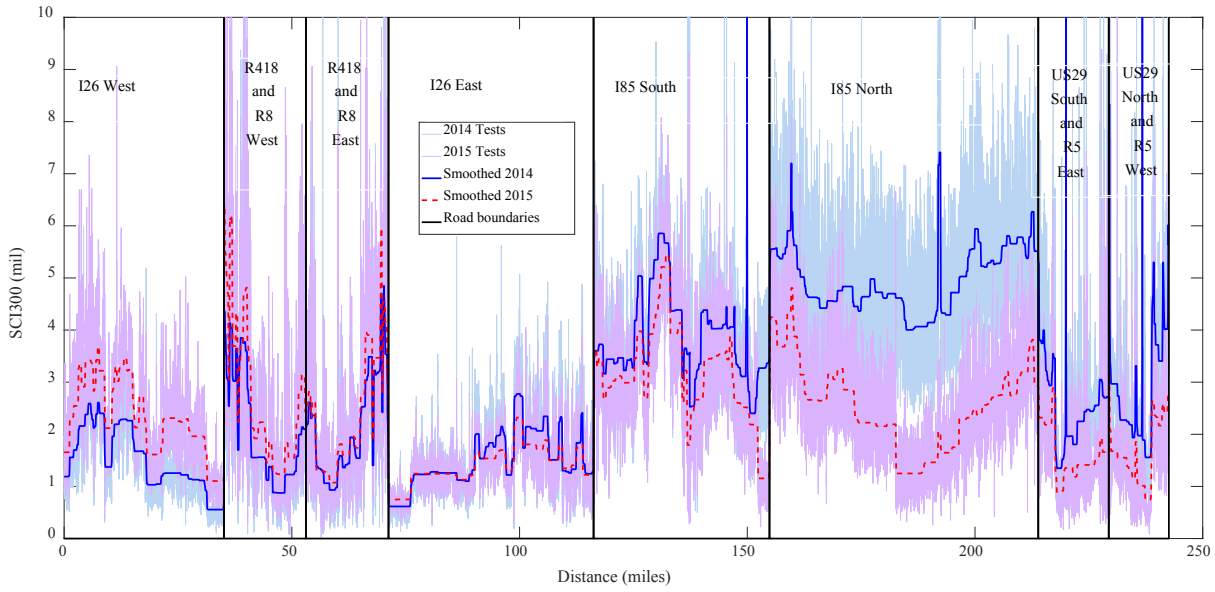

Figure 12. Long-term repeatability of the TSD on roads tested in South Carolina.

COMPARISON OF TSD AND FWD MEASUREMENTS

The FWD is a widely used and accepted device for the structural evaluation of pavement sections. Between 2006 and 2008, the Virginia Department of Transportation (VDOT) performed a network-level structural evaluation with the FWD at 0.2-mile intervals on the state's interstate network. This evaluation was used to compare TSD and FWD test results on a 74-mile section of I-81. The TSD was also used to test other interstate sections (namely on I-64 and I-95); however,

the selected I-81 section includes a rehabilitated section that has detailed before and after FWD tests that are relevant to the comparison of the TSD to the FWD. Figure 13 shows both TSD and FWD D0 (deflection at the center of the applied load). The TSD measurements shown in the figure are averaged over 0.2 mile to match with the 0.2-mile testing interval of the FWD. Note that the scale of the measurements is different for each device; however, the measurement trends are similar (TSD measurements where not corrected for temperature in this comparison).

The section between mileposts 214 and 218 was rehabilitated (using a variety of recycling methods) in 2011, and detailed FWD data are available for this segment before and after rehabilitation. FWD data between 2007 and 2010 show that the structural condition of the section did not change significantly in the 3- to 4-year period. (If any change is observed, the data suggest that the pavement slightly strengthened during that time period, although no treatment was applied, with the average temperature-corrected 2010 D0 being 10.86 mil and the average temperature-corrected 2007 D0 being 12.17 mil). The rehabilitation work improved the structural condition of the pavement section as reflected in the decreased D0 of FWD measurements performed in 2011, 2012, and 2013. The TSD-calculated D0 from the 2015 test follows the trend of the FWD results of 2011, 2012, and 2013, suggesting that the improved structural condition of the pavement section was also captured by the TSD measurements.

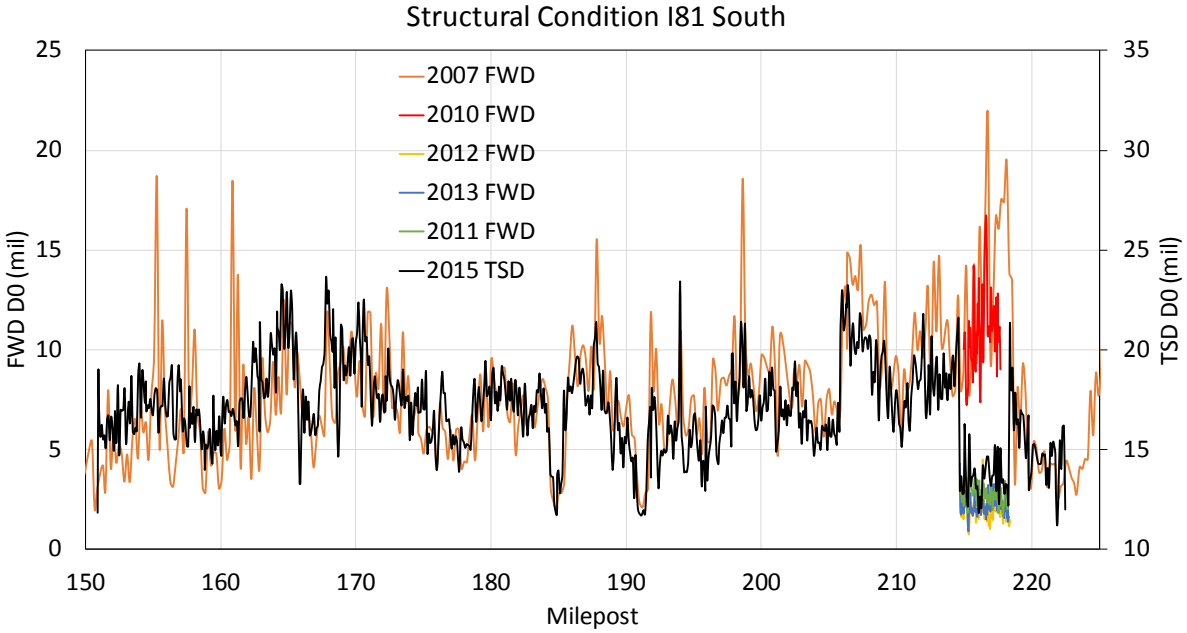

Figure 13. Comparison of TSD and FWD D0 on I-81 South in Virginia.

The section between mileposts 150 to 162 is another interesting one showing a difference between the TSD and FWD. The section is a composite pavement that underwent a series of rehabilitations, most notably jacking and grouting of the concrete slab in 2013 along with mill and overlay work that ranged from 3 to 5.5 inches. The weak spots measured by the FWD (high peaks observed in the plot) were strengthened by this series of rehabilitations, and this strengthening is

reflected in the TSD data. In summary, the results obtained on this section of I-81 show that the TSD and FWD measurements have similar trends and that changes in the structural condition, mainly improvement by rehabilitation, are reflected in the TSD measurements.

COMPARISON OF TSD MEASUREMENTS WITH PMS DATA

Comparison with Overall Surface Condition Data

Pavement condition data for some of the sections tested were obtained from three of the participating states: Pennsylvania, Illinois, and Virginia. Pennsylvania uses the Overall Pavement Index (OPI), which ranges from 0 to 100 (0 failed and 100 new), to summarize the condition of pavement sections. Virginia uses the Critical Condition Index (CCI), which also ranges from 0 to 100, while Illinois uses the Condition Rating Survey (CRS), which ranges from 0 to 10. The OPI and CCI are recorded at a 1-unit resolution, while the CRS is recorded at a 0.1-unit resolution. Figure 14, Figure 15, and Figure 16 show the structural condition measured by the TSD compared to the OPI, CRS, and CCI, respectively. For all three figures, there is practically no relationship between the TSD measurements and the respective surface condition index. For example, Figure 14 shows Pennsylvania data; the road section between mile 18 and 22 and the road section between mile 35 and 40 have similar SN_{eff} values (around 3). However, the two sections have significantly different OPI values, with an average of 95 for the first section and an average of 65 for the second section. This shows that the observed surface condition of the pavement is not representative of the structural condition of the pavement as measured by the TSD. A typical example of how the surface condition in the PMS and the structural condition obtained from the TSD can give different results would be a relatively structurally weak pavement section that has just been resurfaced with a 2-inch mill and overlay. The CCI for this pavement section would be close to 100, which is very good, while the structural condition is poor (weak pavement). Alternatively, a structurally strong pavement section could have an old surface that experienced top-down cracking, and therefore have fair or poor CCI. This shows the importance of evaluating the structural condition, and that the TSD provides information that is currently not available as part of SHAs' PMSs.

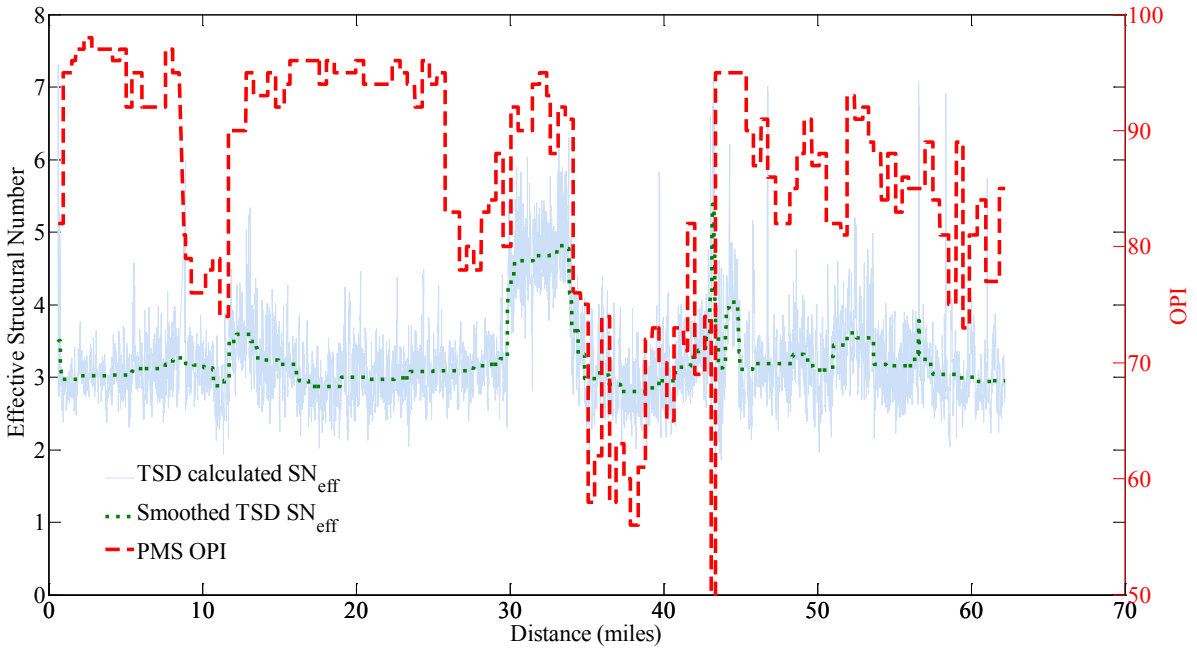

Figure 14. Comparison of TSD calculated SN_{eff} and PMS OPI in Pennsylvania.

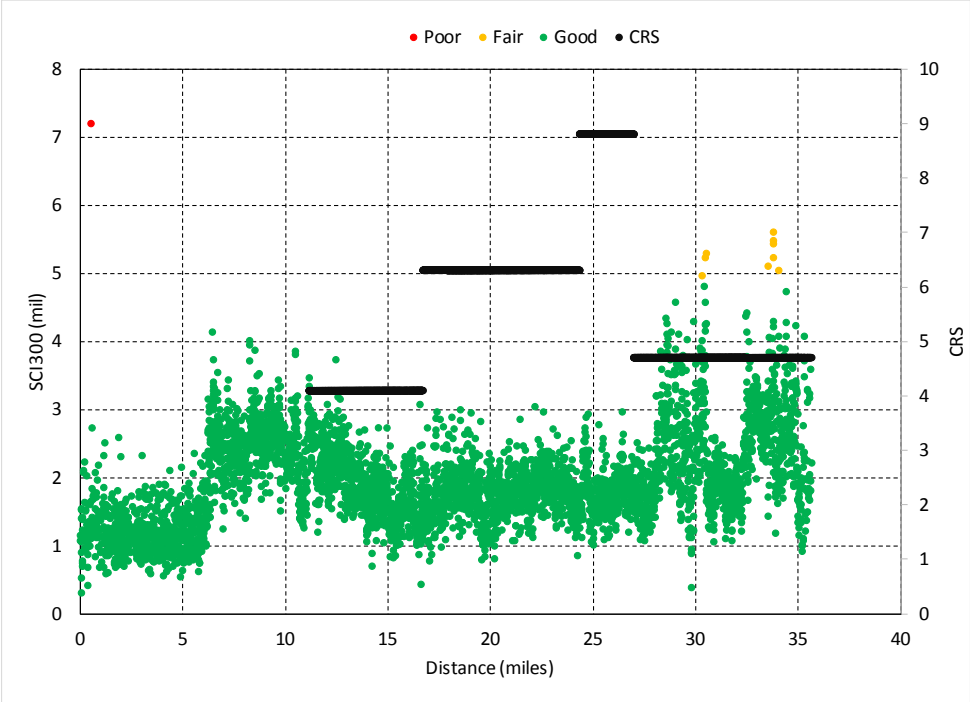

Figure 15. Comparison between TSD SCI300 and PMS CRS in Illinois.

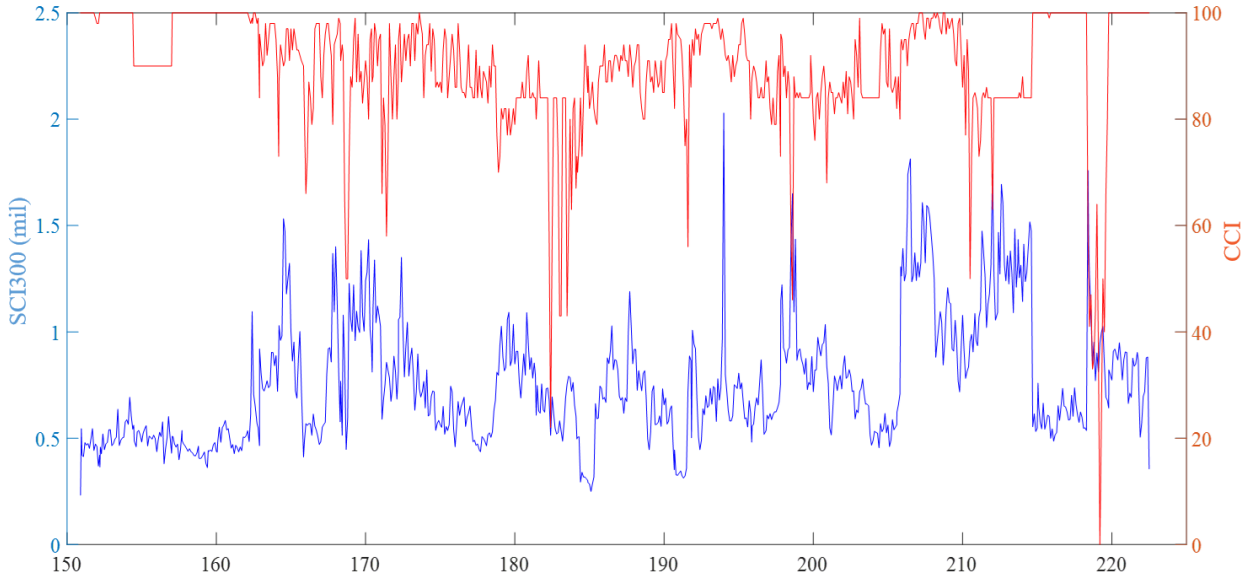

Figure 16. Comparison between SCI300 and CCI in Virginia.

Comparison with Layer Coefficient Estimated Structural Number

The comparison between TSD-calculated SN_{eff} and SN_{eff} estimated based on the American Society of State Highway and Transportation Officials (AASHTO) 1993 layer coefficient approach was performed for data from Pennsylvania and Idaho. The Pennsylvania PMS records a calculated SN_{eff} for their pavement sections based on layer thickness, layer structural coefficient, and layer structural coefficient reduction as a function of layer age. The calculation is similar to the AASHTO 1993 design method except that the layer coefficients are reduced as the layer ages. Figure 17 shows a significant discrepancy between the TSD-calculated SN_{eff} and the Pennsylvania PMS-calculated SN_{eff} between mile 12 and mile 25. This shows that the PMS-calculated SN_{eff} does not reflect the actual pavement structural condition. The SN_{eff} approach used in the PMS makes assumptions about how the structural condition of the pavement will deteriorate; however, the actual field deterioration can be different than assumed. On the other hand, the TSD takes measurements that are directly related to the actual structural condition of the pavement. Note that the capability of the TSD to represent the true pavement structural condition has been validated with FWD results (see Figure 13 and Flintsch et al. 2013) and with instrumented pavement sections by Rada et al. (2016).

Figure 18 reinforces the argument that the structural condition cannot be obtained from currently available PMS data. The figure shows an example of a road in Idaho where detailed layer thickness and composition were collected using ground penetrating radar (GPR) in conjunction with the TSD testing (both at 10-m intervals). The layer thickness and composition were used to calculate the AASHTO 1993 SN_{eff} using a layer coefficient of 0.44 for the asphalt layer and 0.25 for the base layer, which represents the as-constructed SN_{eff}. The SN_{eff} was also calculated from the TSD data using the Rohde (1994) method (equation 7). Again, the TSD SN_{eff} is different from

the one estimated based on layer thickness information. This shows the importance of getting actual field measurements to characterize the structural condition and not relying on design parameters that are not representative of the true current structural condition.

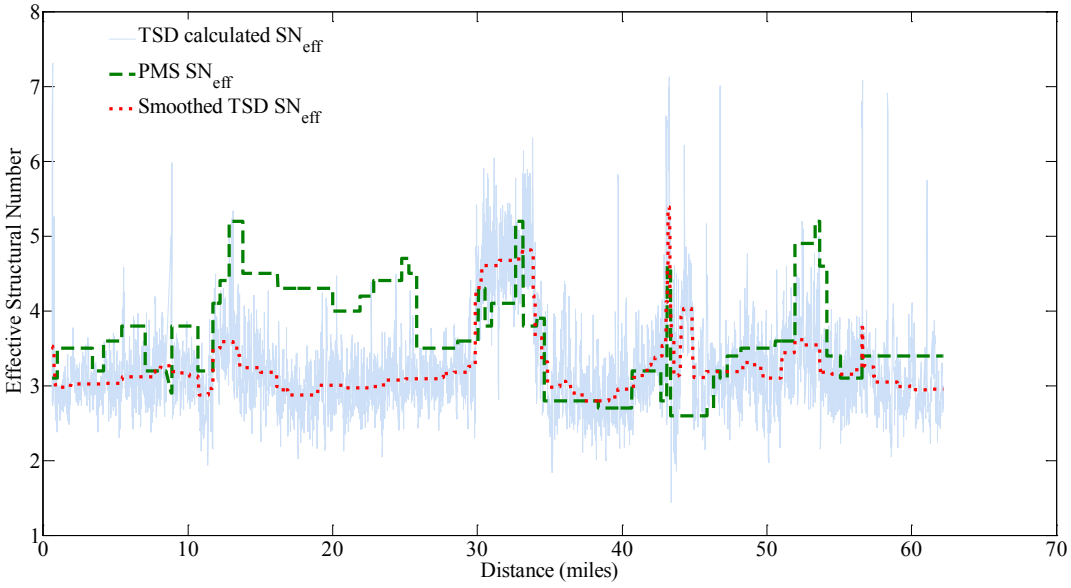

Figure 17. TSD *SN*$_{eff}$ and Pennsylvania PMS *SN*$_{eff}$.

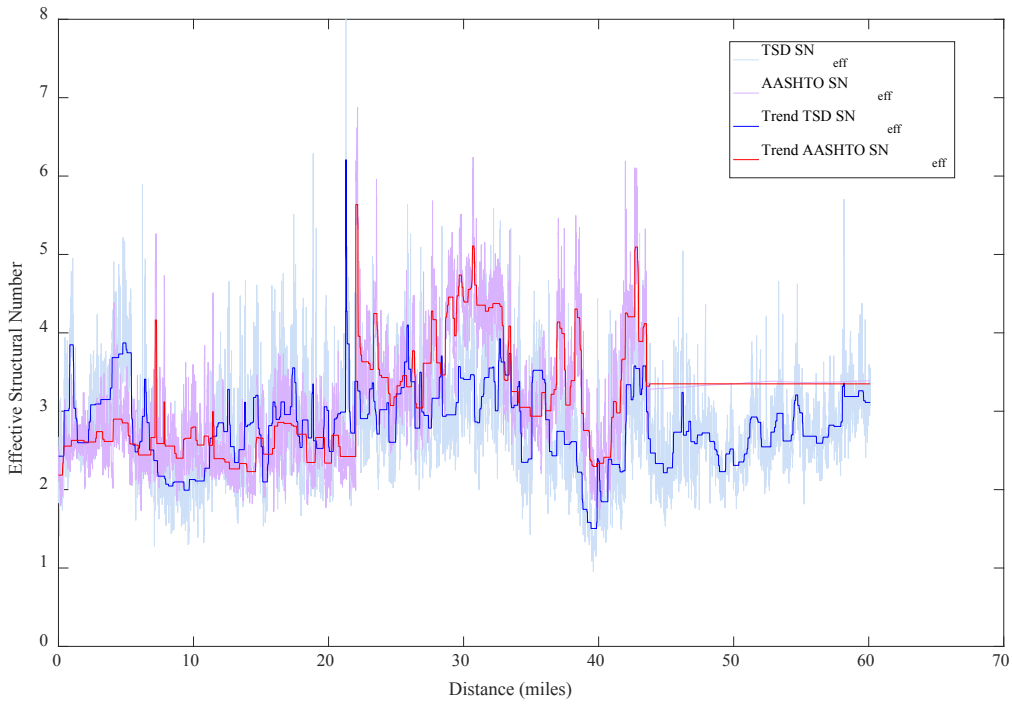

Figure 18. TSD calculated *SN*$_{eff}$ and AASHTO layer thickness and coefficient *SN*$_{eff}$.

Comparison with Detailed Fatigue Cracking Data

The Virginia PMS records pavement fatigue cracking at three severity levels (from 1 to 3, with 1 being least severe and 3 most severe) at 0.1-mile intervals. Figure 19 shows little correlation between SCI300 and Severity 1 fatigue cracking on I-81. Most sections on I-81 had zero to little measured fatigue cracking—mostly Severity 1 (see Figure 19). The same observation was also made for I-64. However, a more significant number of sections on I-95 had non-zero measured fatigue cracking. Figure 20 shows the Severity 1 fatigue cracking for the three interstate roads. More than 90% of I-64 and I-81 sections had practically no fatigue cracking compared with 50% of I-95 sections. Between 2011 and 2012, most of I-95 had received a 3- to 4.5-inch mill and overlay, but fatigue cracking reappeared rather quickly. On the other hand, some sections on I-81 and I-64 received a mill and overlay treatment and are still performing well in terms of fatigue cracking. Furthermore, I-81 sections that have not received a mill and overlay between 2007 and 2014 are still generally performing well in terms of fatigue cracking. Figure 21 shows the distribution of temperature-corrected TSD SCI300 for the three roads. The I-95 distribution shows higher SCI300 values and as such a weaker pavement. This sheds light on why more cracking is observed on I-95. Although a large portion of it had been recently resurfaced, these portions are still relatively weak, which is leading to fatigue cracking in a short time period. A subpopulation on I-95 has low SCI300 values, but this consists of a strong composite pavement. Figure 22 shows the distribution of FWD SCI300 (collected between 2006 and 2007 and not temperature corrected) for I-81 and I-95, which also shows that I-95 has in general higher SCI300 values. The Spearman rank correlation between SCI300 and Severity 1 fatigue cracking was 0.20 for I-81, and 0.16 for I-95, and 0.40 for both combined. These results suggest that, in general, weaker pavement sections will exhibit more cracking (I-95 weaker than I-81); however, this is a very broad trend and observed cracking cannot be a substitute for pavement structural condition measurements (for both I-81 and I-95, cracking does not correlate well with structural condition). Also, surface cracking is a lagging indicator, which limits cost-effective alternatives that would otherwise have been possible if the structural deterioration is identified well before the fatigue cracks appear on the surface.

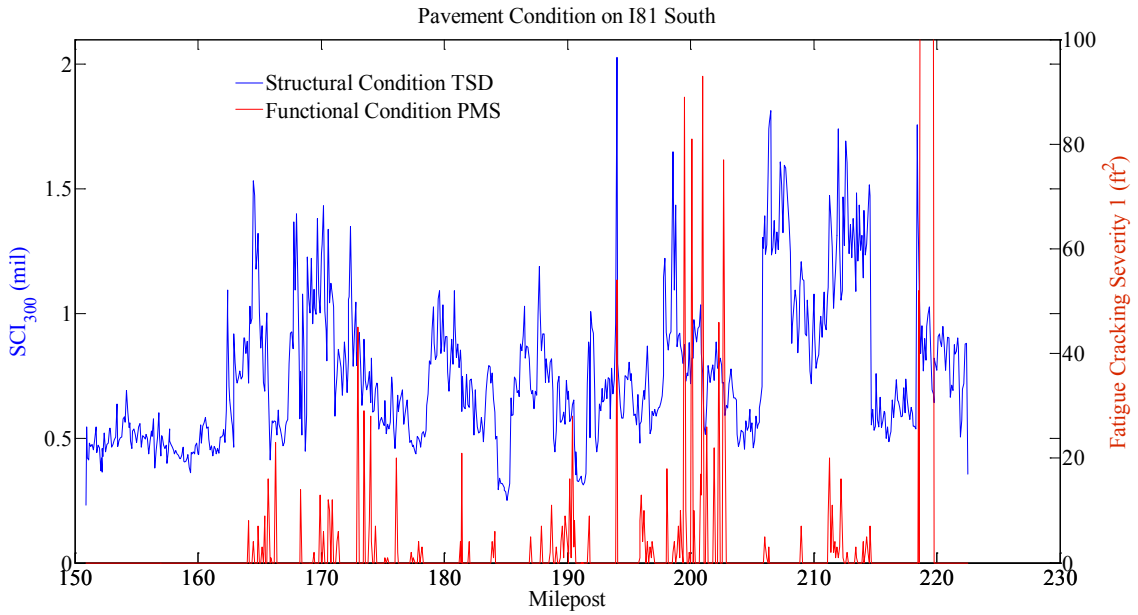

Figure 19. Comparison of TSD SCI300 and Severity 1 fatigue cracking on I-81 South.

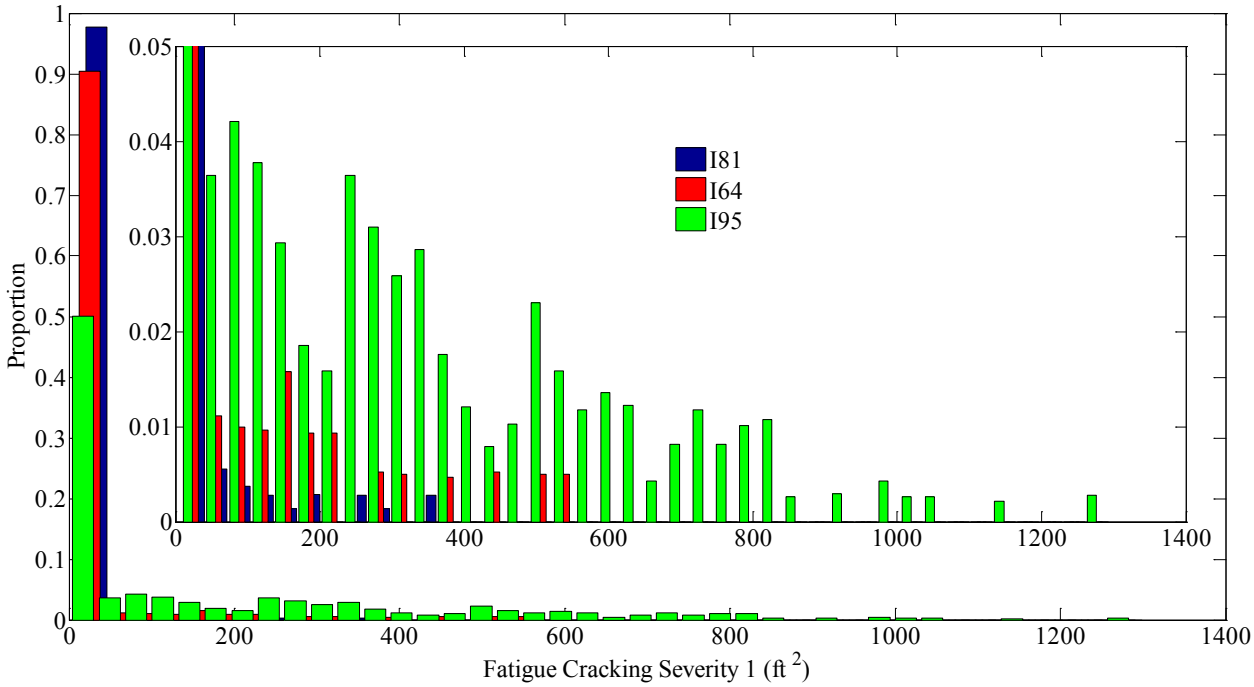

Figure 20. Observed frequency of Severity 1 fatigue cracking on tested interstate sections in Virginia.

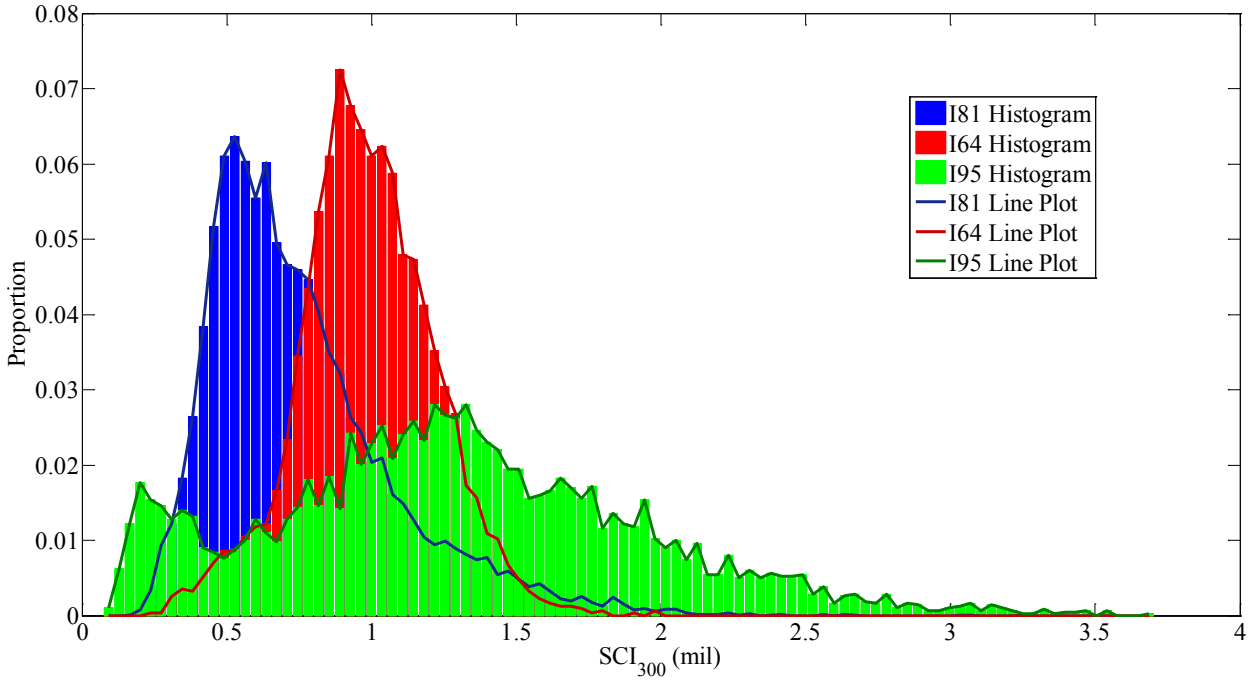

Figure 21. Observed frequency of TSD SCI300 on tested interstate sections.

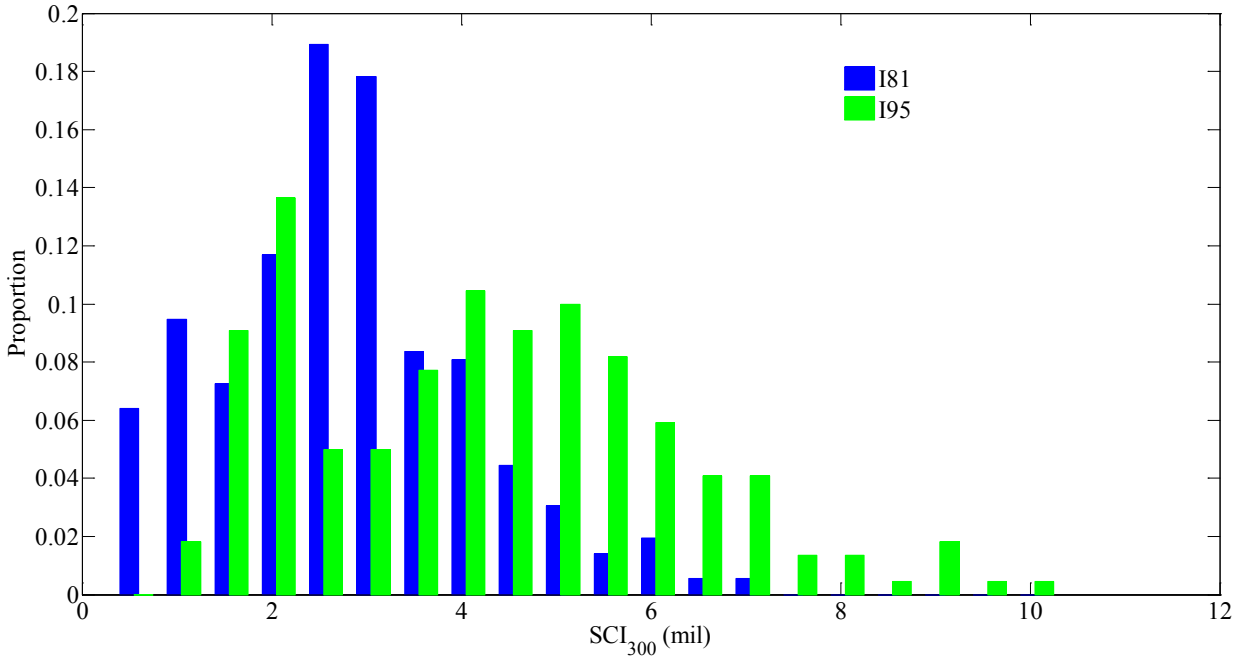

Figure 22. Observed frequency of FWD SCI300 on I-81 and I-95 sections.

FRAMEWORK FOR ROAD CLASSIFICATION INTO GOOD, FAIR, AND POOR STRUCTURAL CONDITIONS

TSD measurements can be used to classify pavement sections into structurally strong, fair, and weak categories (good, fair, and poor). The definition of good, fair, and poor can be based on different parameters. Figure 23 shows an example of such a classification of secondary roads in Virginia based on the thresholds reported in Table 5. Another method to determine thresholds could be based on percentiles of the cumulative distribution of the measurements. Figure 24 shows a classification based on percentiles, where the 25th percentile is used to separate good and fair sections, and the 90th percentile is used to separate fair and poor sections of a road near Carson City in Nevada (seeFigure 25). The classification could be used to determine the required type of treatments, if any. For example, identified poor sections could be assigned as candidate sections for some structural treatments; sections identified as fair could be assigned as candidates for lighter treatments, such as preventive maintenance if needed based on surface distress measurements, or no treatment. For comparison, the classification based on the thresholds reported in Table 5 is shown in Figure 26.

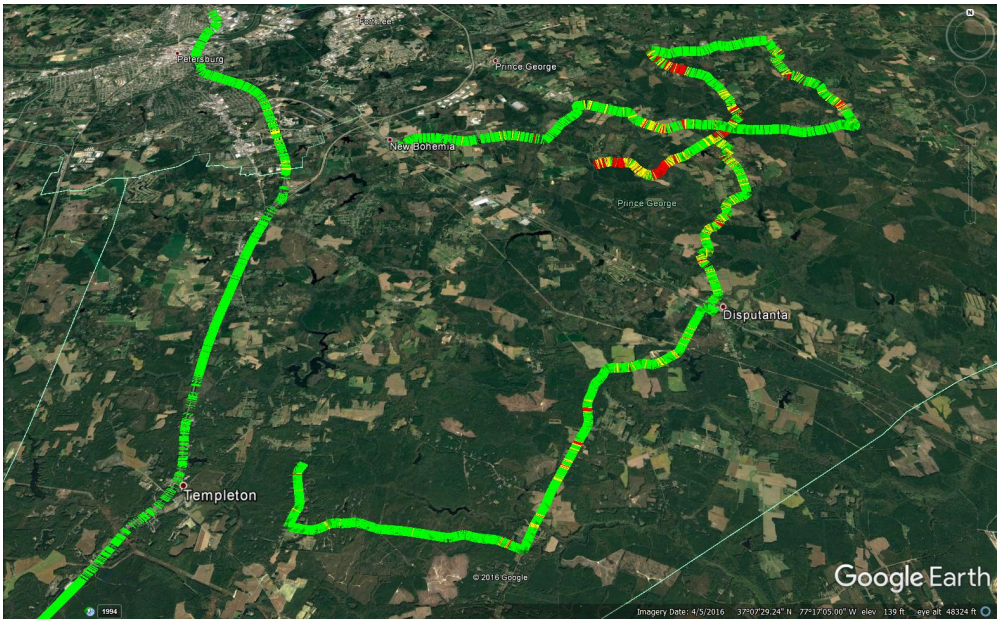

Figure 23. Map. Identified good/strong (green) and poor/weak (red) sections (© 2016 Google Image Landsat/Copernicus).

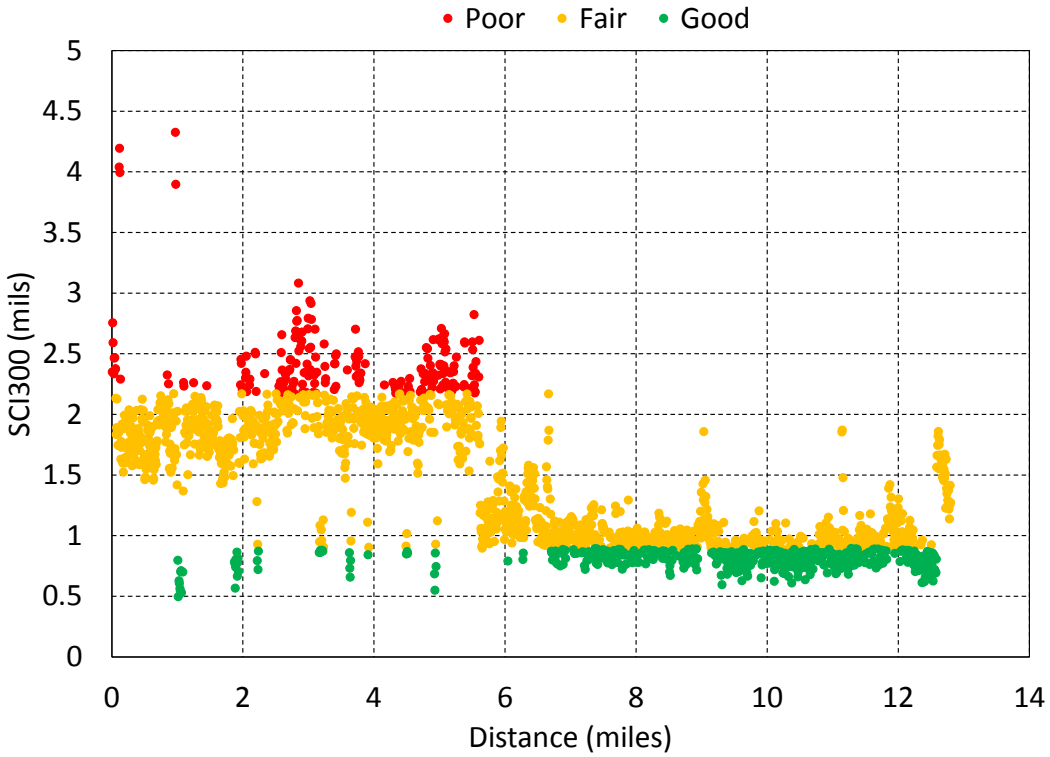

Figure 24. Structural condition classification based on percentile of SCI300 distribution.

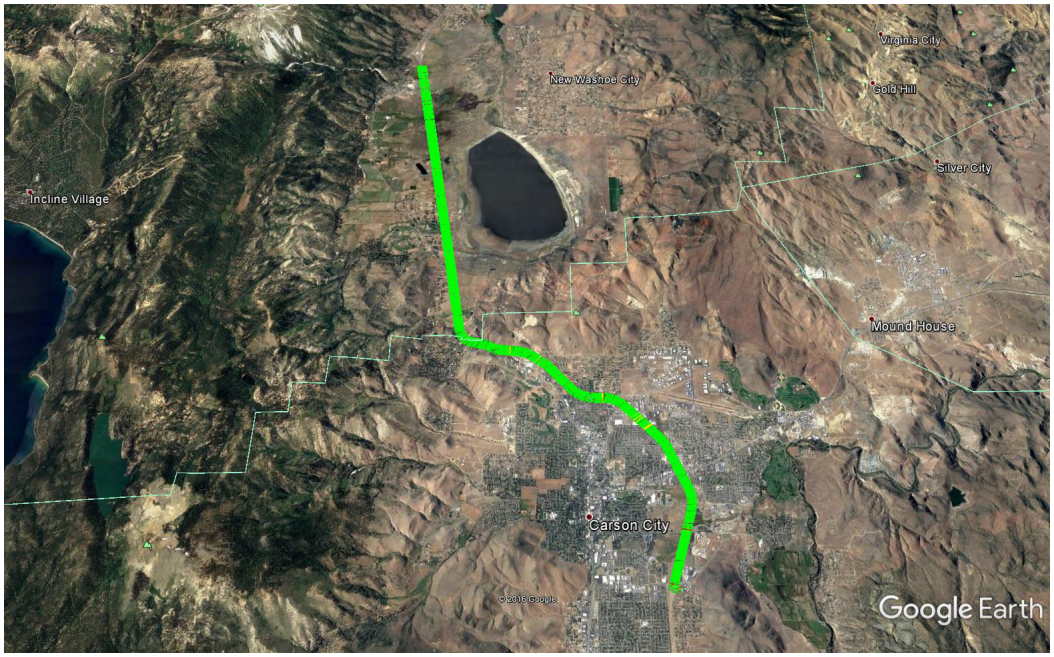

Figure 25. Google Earth view of tested road in Figure 24.

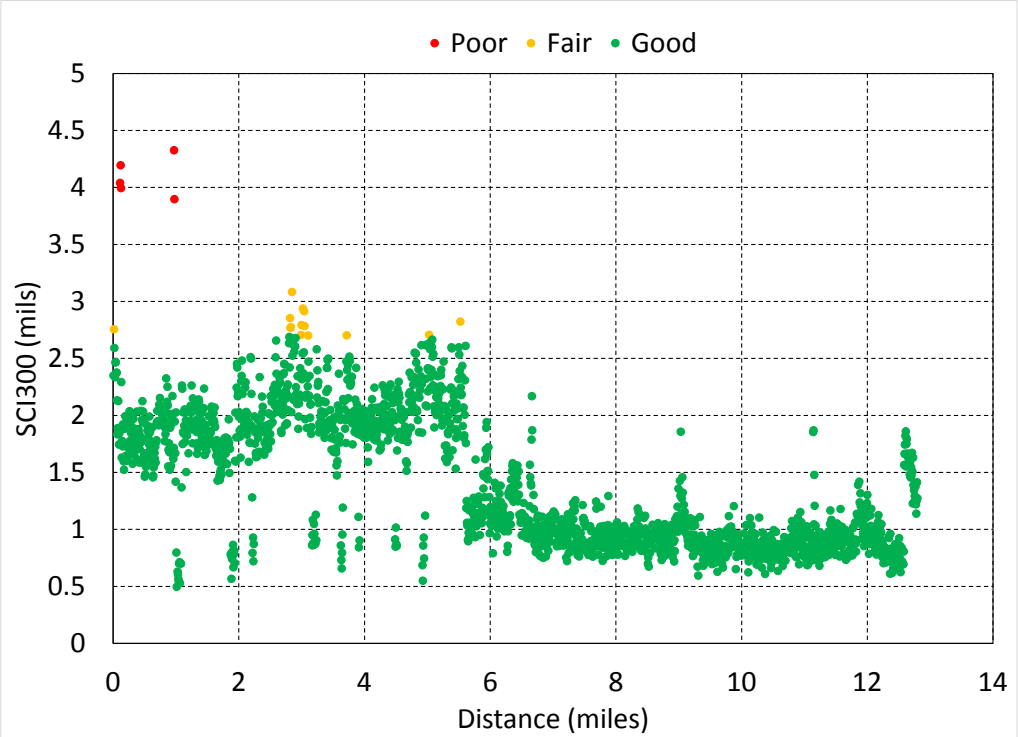

Figure 26. Structural condition classification based on SCI300 thresholds from Table 5.

INCORPORATING STRUCTURAL CONDITION INFORMATION INTO THE PMS DECISION PROCESS

VDOT uses a set of pavement management decision matrices with distresses as inputs and treatment activities as outputs. The matrices are separated based on the following roadway classifications: Interstates, Primary Routes, Secondary Routes, and Unpaved Roads, in addition to the following pavement types: bituminous-surfaced (BIT), bituminous-surfaced composite pavements (with jointed concrete pavement below the surface, BOJ), bituminous-surfaced composite pavements (with continuously reinforced concrete pavement below the surface, BOC), continuously reinforced concrete (CRC), and jointed concrete pavements (JCP). Additionally, updated cost estimates per mile for each treatment are available for each road category. The decision process is a two-phase approach (Figure 27). In 2008, this two-phase approach was modified to include structural condition and truck traffic volumes, and the enhanced decision tree was integrated into the process. One of the main features of the approach is that the addition of the pavement structural information did not alter the core of the decision process already in place but provided an additional step that can be used when pavement structural condition is available. If structural information becomes unavailable, the decision process can revert to the core process already in place. VDOT currently uses the following five treatment categories (from do nothing to heavier treatments): Do Nothing (DN), Preventive Maintenance (PM), Corrective Maintenance (CM), Rehabilitation Maintenance (RM), and Reconstruction (RC). At the preliminary treatment stage, one of these five categories is selected based on the condition index and the decision matrices. In the enhanced decision process, based on the structural condition (and traffic level and

construction history), the selected preliminary treatment can be either retained or modified to a heavier or lighter treatment.

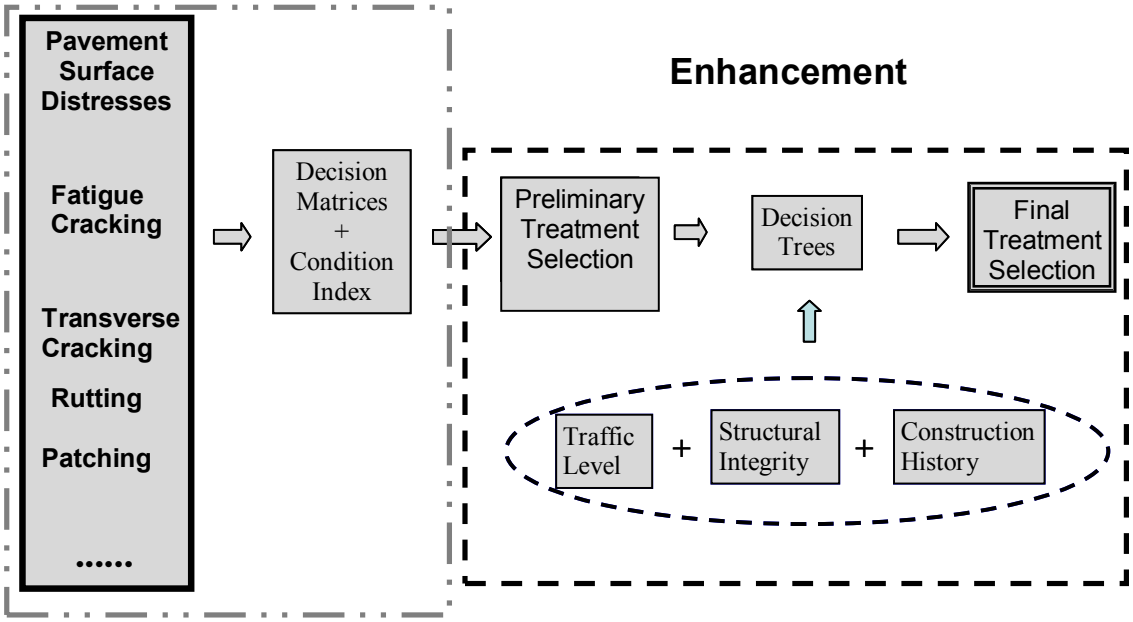

Figure 27. DOT two-phase decision process (Virginia Department of Transportation, 2008).

Example of PMS Decision Process with TSD-Derived Structural Condition

This section presents an example of how the structural condition will affect the triggered maintenance category at the network-level analysis for the tested I-81 section in Virginia. The approach is based on the CCI recommended treatment used by VDOT. It should be noted that in the actual VDOT decision process, the different distresses—e.g. cracking, rutting, etc.—are used to trigger the maintenance category and the CCI is used as an additional filter. Here the process is simplified for a clearer exposition. Figure 28 shows the maintenance categories as a function of CCI for the different road systems used by VDOT. This example uses I-81 and therefore the triggered categories for the interstate road system are used. The different treatment categories are codified with a numerical value as follows: DN = 1, PM = 2, CM = 3, RM = 4, and RC = 5. After the triggered maintenance category is obtained from the CCI, the structural condition information is used to potentially bump up the triggered maintenance category. The structural condition information used is the one obtained from the SCI300 with thresholds determined from Table 5. The approach to bump up the triggered maintenance category is as follows: if all the SCI300 measurements in the pavement section have good structural condition, keep the maintenance category triggered by the CCI with a maximum category of 3; if there are SCI300 measurements within the pavement section that are classified as fair, bump up the maintenance category triggered by the CCI by one not to exceed a maintenance category of 5; if there are SCI300 measurements within the pavement section that are classified as poor, bump up the maintenance

category triggered by the CCI by two not to exceed a maintenance category of 5 and a minimum category of 4.

In total there are 747 0.1-mile sections tested in I-81. The triggered maintenance categories obtained before and after taking into account the structural condition are shown in Figure 29. Of the 747 sections, 66 (8.8%) had the triggered maintenance category bumped up; 50 by one, and 16 by 2. The total number of sections in each maintenance category before and after incorporating the structural condition are DN 384 before, 345 after; PM: 338 before, 347 after; CM: 6 before, 25 after; RM: 14 before, 23 after; RC: 5 before, 7 after. The number of sections in the DN categories decreased, while the number of sections in all other categories increased. Again, this example is simplified, and other factors such as traffic level and pavement age can be considered (as is done by VDOT). It is expected that different state highway agencies will tailor their approach for their specific needs.

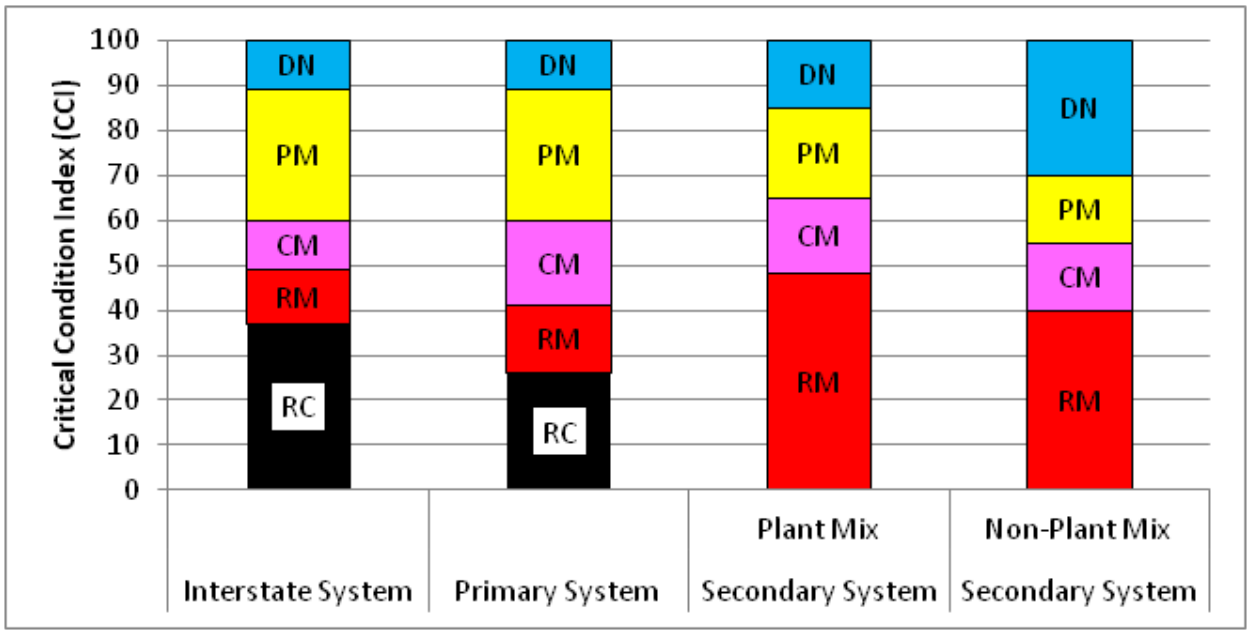

Figure 28. Maintenance activities for each road system (from Chowdhury, 2008).

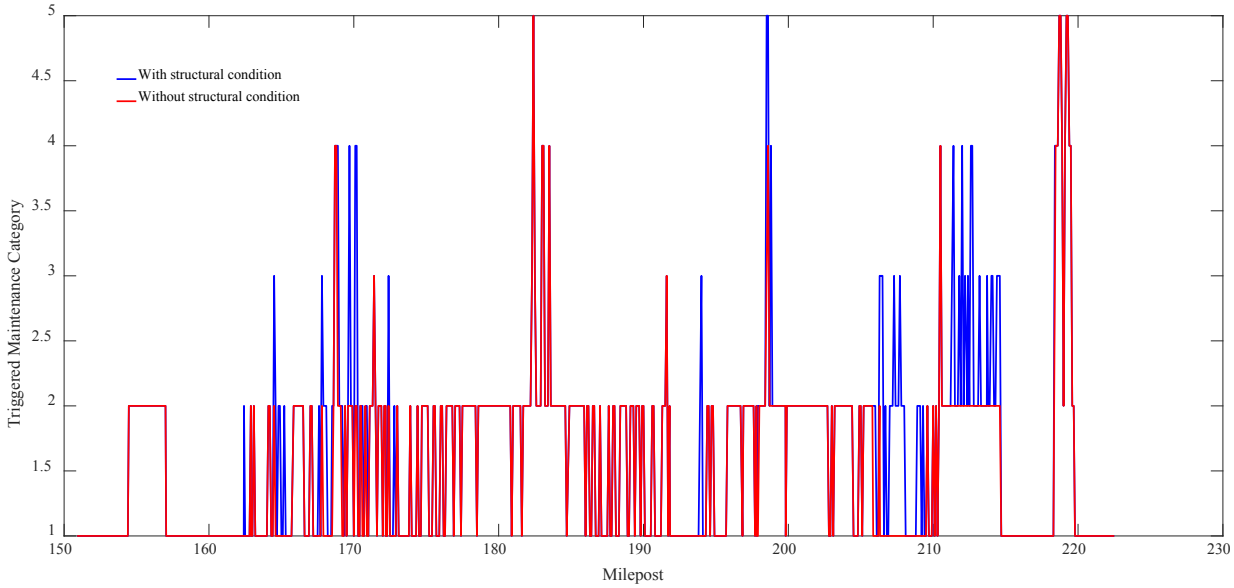

Figure 29. Triggered maintenance category before and after structural condition consideration.

CONCLUSION

This report summarizes the results and findings from the TSD testing performed in nine SHAs that participated in the transportation pooled fund study "Demonstration of Network Level Pavement Structural Evaluation with Traffic Speed Deflectometer." Companion reports, documenting SHA-specific data analysis, findings, and recommendations have also been prepared and provided to each participating SHA. Based on the findings from this effort, the following conclusions are made:

1. The short- and long-term repeatability of the TSD is generally good. Repeated measurements performed on consecutive days or in two different years followed similar trends. However, work is needed to more accurately account for the effect of temperature on TSD measurements.
2. A comparison of the TSD with the FWD on a section of I-81 in Virginia showed that the two devices followed similar trends along the tested road. Rehabilitation work performed on parts of the tested road suggests that the structural improvement is reflected in FWD testing. TSD measurements followed the trend of FWD measurements, which suggests that the structural improvement is also picked up by TSD measurements.
3. Comparison between TSD indices and PMS surface condition data suggests little relationship. Detailed investigation between TSD SCI300 and PMS-recorded fatigue cracking shows that structurally weaker pavement sections in general exhibit more fatigue cracking. However, this is a broader trend and observed fatigue is not a robust indicator of the pavement structural condition.

4. State highway agencies can choose from a number of approaches to use for classifying the structural condition of their pavement network. A mechanistic approach based on tensile strain at the bottom of the asphalt layer developed in Rada et al. (2016) is presented and preliminary values for thresholds are given. An alternative approach based on percentile from the cumulative distribution of SCI300 is also discussed. Finally, SN_{eff} derived from TSD data could also be used. The choice of which approach to use will ultimately be made by the individual SHA to best meet their needs and capabilities.
5. A framework to incorporate the TSD-measured structural condition within a SHA's PMS is presented. The framework is based on the current two-stage approach followed by Virginia DOT. In the first stage, the triggered maintenance category in the PMS is based on surface condition. In the second stage, the triggered maintenance category is combined with structural condition information to determine the final recommended maintenance category. An example of the two-stage approach on 741 0.1-mile sections on I-81 is presented, and a total of 66 sections had the final suggested maintenance category bumped up from the original triggered maintenance category based solely on pavement surface condition.

REFERENCES

AASHTO (1993). AASHTO Guide for Design of Pavement Structures, American Association of State Highway and Transportation Officials, Washington, D.C.

Asphalt Institute. (1982). *Research and Development of the Asphalt Institute's Thickness Design Manual (MS-1)*, Research Report No. 82-2, 9th edition.

Chowdhury, T. (2008). *Supporting Document for the Development and Enhancement of the Pavement Maintenance Decision Matrices Used in the Needs-Based Analysis*. Virginia Department of Transportation, Richmond, VA.

Finn, F.N., Saraf, C., Kulkarni, R., Nair, K., Smith, W., & Abdullah, A. (1977). The use of distress prediction subsystems for the design of pavement structures. In *Proceedings of the 4th International Conference on the Structural Design of Asphalt Pavements* (pp. 3–38), Vol. I, August. Ann Arbor, MI: University of Michigan.

Flintsch, G.W., Katicha, S.W., Bryce, J., Ferne, B., Nell, S., and Diefenderfer, B. (2013). *Assessment of Continuous Pavement Deflection Measuring Technologies*, Second Strategic Highway Research Program (SHRP2) Report S2-R06F-RW-1. Transportation Research Board of The National Academies, Washington, D.C.

Jorgen Krarup, Traffic Speed Deflectometer, FWD User´s Group, Sacramento, California, USA, October 16, 2012.

Lukanen, E.O., Stubstad, R., and Briggs, R. (2000). *Temperature Predictions and Adjustment Factors for Asphalt Pavement*. FHWA-RD-98-085, Federal Highway Administration, McLean, Virginia, USA.

Pedersen, L., Hjorth, P. G., and Knudsen, K. (2013). *Viscoelastic Modelling of Road Deflections for use with the Traffic Speed Deflectometer*. Kgs. Lyngby, Technical University of Denmark. (IMM-PHD-2013; No. 310).

Rada, G. R., Nazarian, S., Visintine, B. A., Siddharthan, R.V., and Thyagarajan, S. (2016). *Pavement Structural Evaluation at the Network Level: Final Report*, FHWA-HRT-15-074. Federal Highway Administration, McLean, Virginia, USA. https://www.fhwa.dot.gov/pavement/pub_details.cfm?id=1000

Rohde, G.T. (1994). Determining pavement structural number from FWD testing. *Transportation Research Record,* No. 1448, pp. 61-68.

Virginia Department of Transportation. (2008). *Supporting Document for the Development and Enhancement of the Pavement Maintenance Decision Matrices Used in the Needs Based Analysis*. Richmond, VA.

APPENDIX A: TSD DATA COLLECTION AND PROCESSING

Greenwood Engineering performed the data collection and processing and provided the processed data in a series of Microsoft® Excel® files that included the collected data and roadway image files collected during testing. Figure 30 shows the naming of the provided files. All files start with the TSD unit number (T7 indicating the seventh TSD produced by Greenwood), the testing date (year/month/day), a file number based on the test sequence on the given day, and file type extension. Table 6 shows the different file types; those highlighted in bold were used to process the data in this report. The file type ".tsd.tsd.xls" is the main data file, containing the chainage (10-m interval), raw deflection velocities, the deflection slopes, the applied dynamic load measured with a strain gauge, and the pavement surface and air temperatures. The file type ".tsd.tsddefl.xls" contains the calculated deflections from the deflection slopes at each of the chainage points. The files ".tsd.gpsraw.xls" and ".gpsimp.xls" contain the GPS coordinates, with gpsraw containing the raw GPS measurements in the time domain and gpsimp containing the interpolated GPS coordinates that match the location of the reported deflections. Data processing combined data from the three files into one Excel file with filenames and .xls extension as follows:

- From .tsd.tsd.xls: Chainage, deflection slope measurements, pavement surface temperature, air temperature, and dynamic load obtained from two strain gauges. The strain gauges were used to normalize the deflection to a standard axle load. This was performed for all testing except the first round of testing in New York in 2013, when the strain gauge was not yet installed. Also, the strain gauge data collected during the Pennsylvania 2015 testing had to be recalibrated with strain gauge data collected from all other 2015 testing.
- From tsd.gpsraw.xls or gpsimp.xls: The GPS coordinates of collected measurements.
- From tsd.tsddefl.xls: The calculated deflections by Greenwood from the deflection slopes. These are provided at 100-mm intervals between 0 mm and 1,500 mm (location from the center of the wheel load).

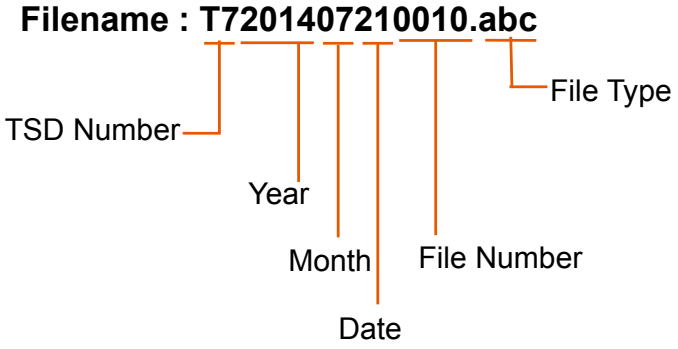

Figure 30. Naming convention for collected files.

Table 6. Provided data files.

File description	File type
Header file	*.tsd.hea.xls*
Event file	*.tsd.evt.xls*
GPS	***.tsd.gpsraw.xls* & *.gpsimp.xls***
Profile	*.pro.xls*
TSD data	***.tsd.tsd.xls***
Deflection data	***.tsd.tsddefl.xls***
Slope data	*.tsd.tsdslope.xls*
International Roughness Index (IRI)	*.iri.xls*
Image Folder	*.row.img*
Right-of-Way pictures	*.row.img.xls*

Once the three files were combined, Google Map links to the location of the performed tests were generated and provided in a table. Table 7 shows an example of generated links for the first round of testing performed in Illinois in 2014. Figure 31 shows an example of a link opened in a Web browser.

Table 7. Map link to location of performed tests in Illinois in 2014.

File No.	File Name	Road Name	Map Link
1.	T7201406280001	I57 South 1	https://goo.gl/maps/n6xCNJT1hBF2
2.	T7201406280002	I57 North 1	https://goo.gl/maps/GQPU6pEsd8n
3.	T7201406280003	I57 South 2	https://goo.gl/maps/yF2tdFLbKFJ2
4.	T7201406280004	I57 North 2	https://goo.gl/maps/79mUCNkq2nr
5.	T7201406280005	I57 South 3	https://goo.gl/maps/bxkQf5jynEN2
6.	T7201406280006	I57 North 3	https://goo.gl/maps/CuU1a2bZu5s
7.	T7201406280019	3602 N Mattis Ave - 900 County Rd 3000 N	https://goo.gl/maps/mop8QzUAWz72
8.	T7201406300001	I57 South – I74 East	https://goo.gl/maps/8x7anEQRdVD2
9.	T7201406300002	I74 West - I57 North	https://goo.gl/maps/RsNGhrQFfN22
10.	T7201406300003	I57 South 4	https://goo.gl/maps/61dwdSK96XT2
11.	T7201406300004	I72 West	https://goo.gl/maps/h7swrWc3ET82
12.	T7201406300005	SR29 East	https://goo.gl/maps/UmevQei4yYk
13.	T7201406300006	US51 North	https://goo.gl/maps/t1tGvDHatcA2

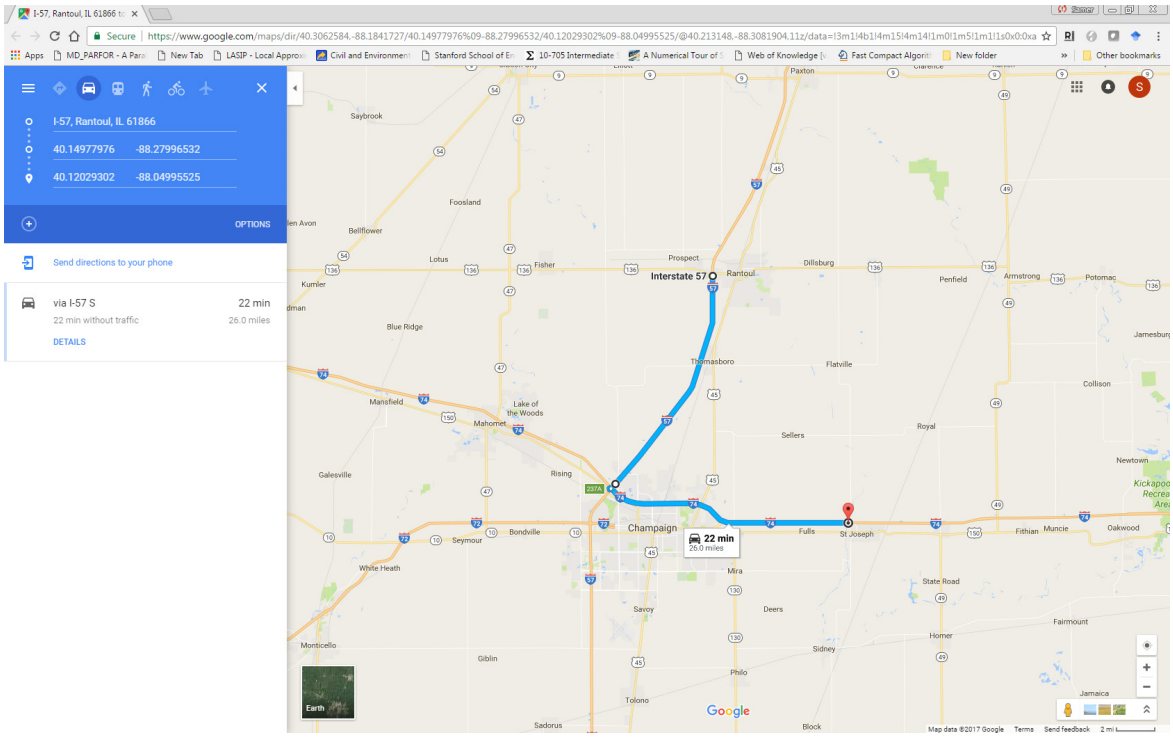

Figure 31. Google Maps© link showing test location on I-57 and I-74 for file "T7201406300001" in Table 2.

Figure 32 shows an example file containing the processed data where most of the column containing the deflection slopes and deflections are hidden for clarity. The SCI300, DSI, Base Damage Index (BDI), and Area Under Pavement Profile (AUPP)were calculated and shown in columns "Z" to "AC" (see Equations A.1 to A.4 at end of Appendix A). The asphalt layer thickness shown in column "AF" was either obtained from the states' pavement management data or assumed to fall in the range of 9 to 16 inches for interstate roads, 6 to 9 inches for primary roads, and 3 to 6 inches for secondary roads. These default values for the different road categories correspond to integer values of 0 for interstate roads, −1 for primary roads, and −2 for secondary roads (e.g., entering a value of 0 in the thickness columns sets the thickness value to the default range of 9 to 16 inches). Negative integer values were used to differentiate between default-assumed values and actual thickness values, which are entered as positive numbers.

The column "Bells Corrected Mid-Depth Temp" which is column "AD" in Figure 32, contains the calculated asphalt layer mid-depth temperature using the BELLS3 equation (Lukanen et al. 2000) (see Equation A.7 at end of Appendix A). The mid-depth temperature is used to normalize the SCI300 and DSI measurements to a reference temperature of 70°F using the procedure developed in Rada et al. (2016) and outlined in the section "Temperature-Correction Procedure." This is performed by first estimating the tensile strain at the bottom of the asphalt layer from SCI300 or DSI measurements, temperature correcting the estimated strain, and finally calculating the

temperature-corrected SCI300 or DSI using the inverse relationship between strain and SCI300 and DSI (see Equation A.6 at end of Appendix A).

This three-step procedure is implemented in columns "AH," "AI," and "AJ" for the DSI, and "AK," "AL," and "AM" for the SCI300 (note that these columns could be slightly different in different files and it is recommended to look at the column headings for confirmation). The columns of temperature-corrected SCI300 and DSI include a color-coded identifier that reflects the estimated structural condition, with green corresponding to good, yellow corresponding to fair, and red corresponding to poor. These are based on thresholds entered in columns "AV" to "AY" (Figure 33) that include suggested default threshold values for different road categories (interstate, primary, and secondary).

The color-coded identifiers, as well as the calculation of SCI300 and DSI, are interactive; changing the threshold values will be reflected in the color of the identifier, and changing the reference temperature, or the asphalt layer thickness will be reflected in the calculated SCI300 and DSI, which will also change the identifier color. Figure 33 shows an example where the thresholds were (arbitrarily) reduced and the color of the identifier changed accordingly (compare with Figure 32).

Columns "AZ" to "BC" show calculated thresholds based on user-selected percentiles, which could also be used to define the good, fair, and poor categories. It should be noted that the user could also decide not to do any temperature correction by entering the value 70 in column "AG." This is not recommended, however. The research team recognizes that the temperature-correction procedure used is still under investigation, and the SHAs might want to evaluate the effect of the procedure on the normalized SCI300 and DSI (as well as the tensile strain at the bottom of the asphalt layer).

The Excel files also include color-coded charts for SCI300 and DSI in separate sheets that are also interactive (i.e., the index values as well as the colors will change). Figure 34 shows an example for SCI300. Finally, Google Earth files with color-coded conditions are also provided. These are, however, not interactive, as they are not linked to Excel files and the colors are not automatically adjusted when the thresholds are changed. The Google Earth files have to be regenerated with the new thresholds. Figure 35 shows the tested Nevada network structural condition as an example in Google Earth. Detailed conditions of a road near Carson City are shown in Figure 36.

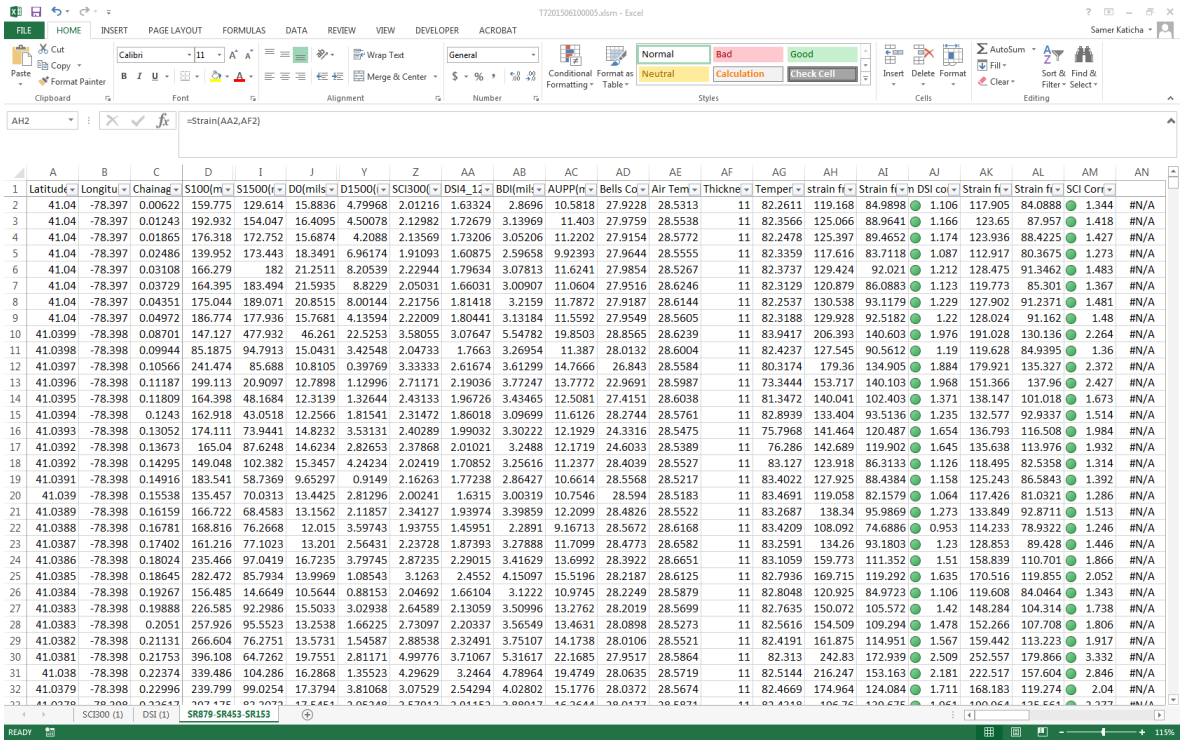

Figure 32. File "T720150100005" from the testing performed in Pennsylvania.

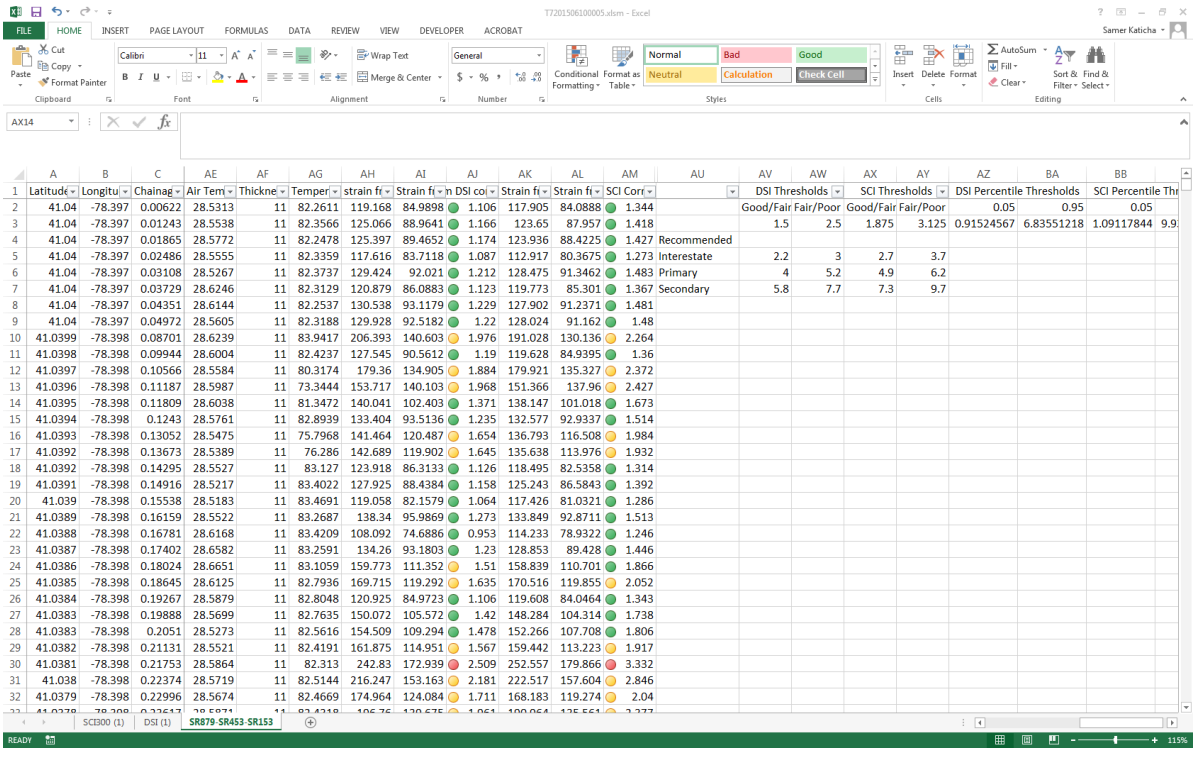

Figure 33. File "T720150100005" from the testing performed in Pennsylvania with modified threshold and corresponding changed condition.

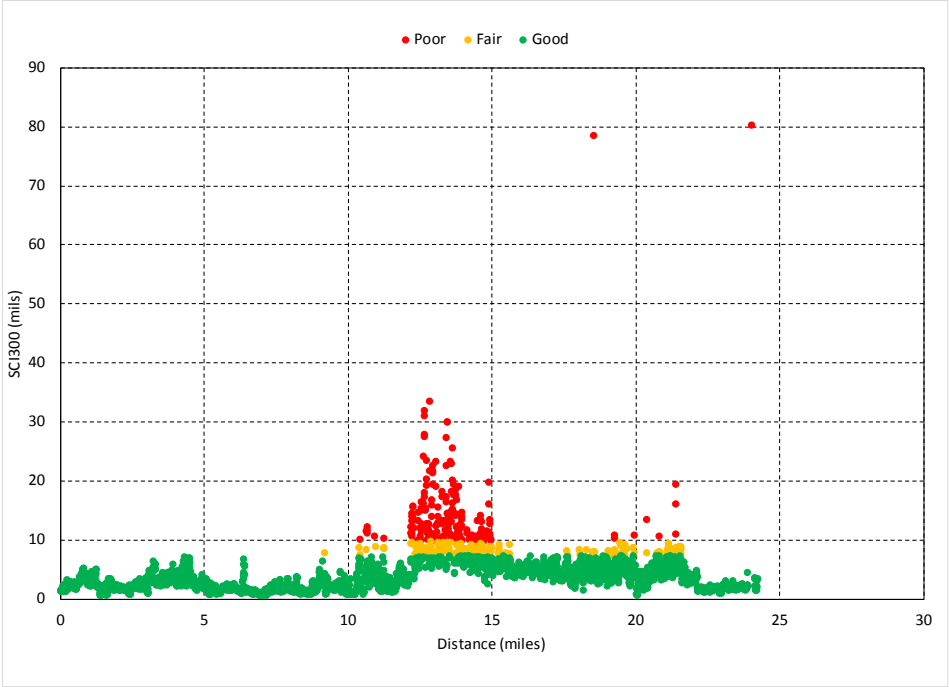

Figure 34. Example color-coded plot of structural condition SCI300 from the file "T720150100005."

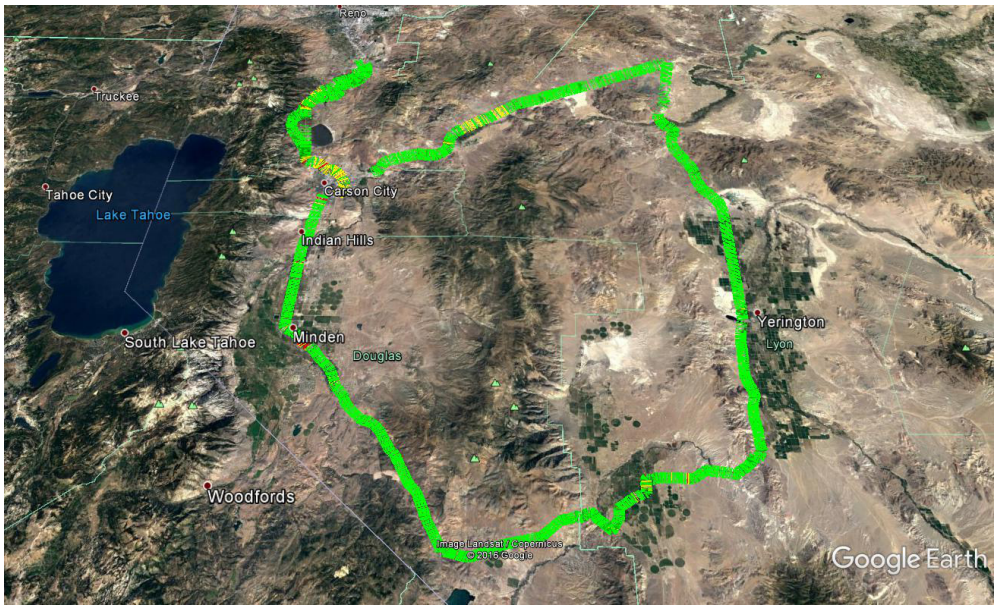

Figure 35. Google Earth color-coded pavement structural condition of tested pavements in Nevada with good (green), fair (yellow), and poor (red) ratings (© 2016 Google Image Landsat/Copernicus).

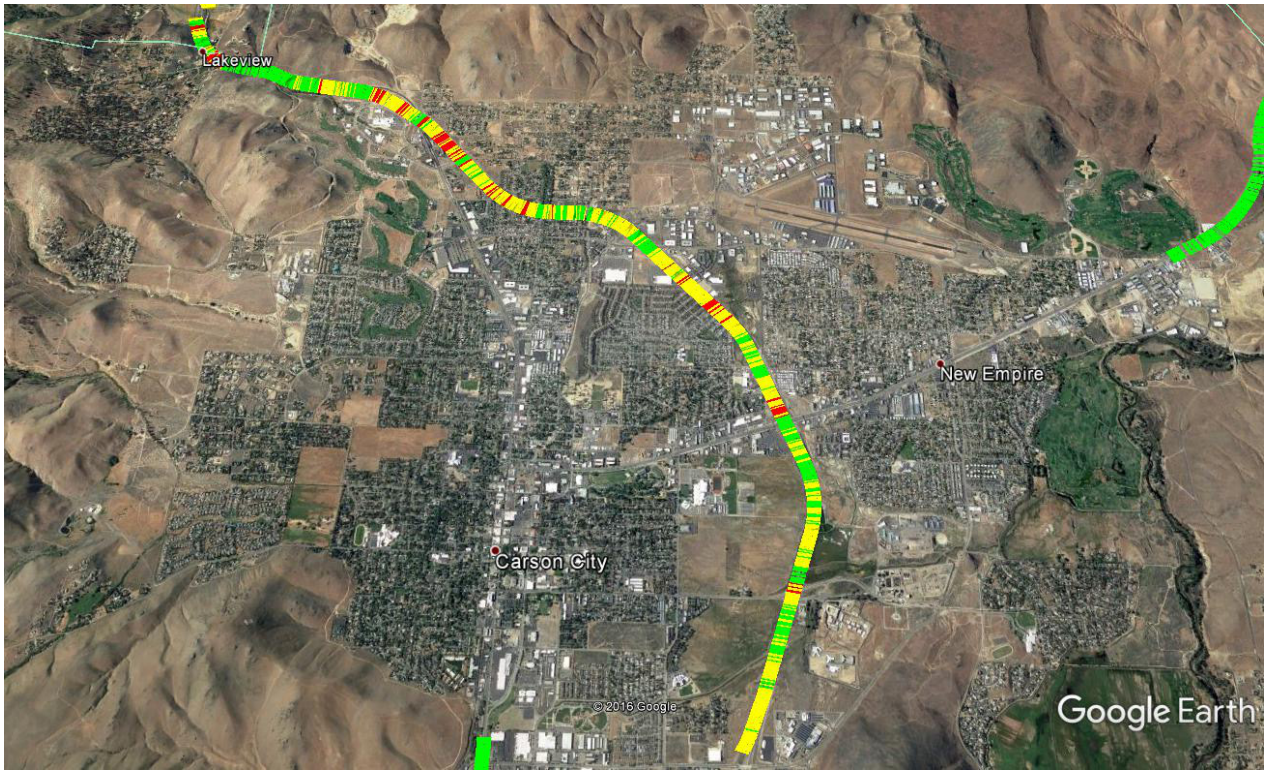

Figure 36. Detail from Figure 5 near Carson City, Nevada (© 2016 Google Image Landsat/Copernicus).

Equations for Indices and BELLS3 Temperature Correction

$$SCI300 = D0 - D300 \tag{A.1}$$

$$DSI = D100 - D300 \tag{A.2}$$

$$BDI = D300 - D600 \tag{A.3}$$

$$AUPP = \frac{5d(0) - 2d(300) - 2d(600) - d(900)}{2} \tag{A.4}$$

$$\varepsilon = a(DSI)^{b} \qquad \varepsilon = a'(SCI\,300)^{b'} \tag{A.5}$$

$$DSI = \left(\frac{\varepsilon}{a}\right)^{\frac{1}{b}} \qquad SCI300 = \left(\frac{\varepsilon}{a'}\right)^{\frac{1}{b'}} \tag{A.6}$$

The coefficients a and b are given in Table 3; a' and b' are given in Table 4.

BELLS3 equation is calculated as follows (Lukanen et al. 2000):

$$T_d = 0.95 + 0.892 \times IR + \{\log d - 1.25\}\{-0.448 \times IR + 0.621 \times (\text{1-day}) + 1.83 \times \sin(\text{hr18} - 15.5)\} + 0.042 \times IR \times \sin(\text{hr18} - 13.5)$$

where:

T_d = pavement temperature at mid-depth d, °C
IR = pavement surface temperature, °C
log = base 10 logarithm
d = mid-depth of the AC layer, mm
1-day = average air temperature the day before testing, °C
sin = sine function on an 18-hr clock system, with 2π radians equal to one 18-hr cycle
hr18 = time of day, in a 24-hr clock system, but calculated using an 18-hr asphalt concrete (AC) temperature rise-and-fall time cycle

APPENDIX B: TSD PROFILOGRAPH

The TSD profilograph was provided to each participating SHA by Greenwood Engineering on a separate USB drive. The profilograph can be used to view the collected IRI, deflection indices, longitudinal profile, IRI, forward-facing images of the tested road, and test location on a map. Figure 37 shows the layout of the profilograph window.

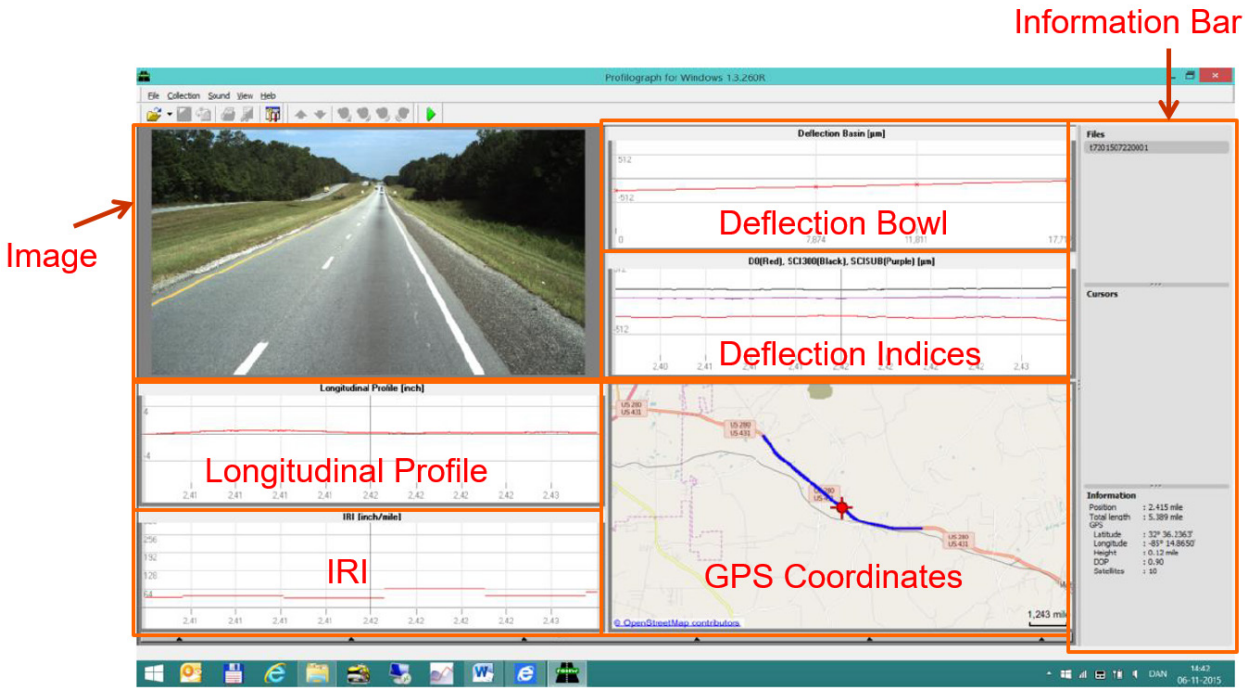

Figure 37. Overview of TSD profilograph.

To launch the profilograph, select the folder TSD Viewer262 as shown in Figure 38.

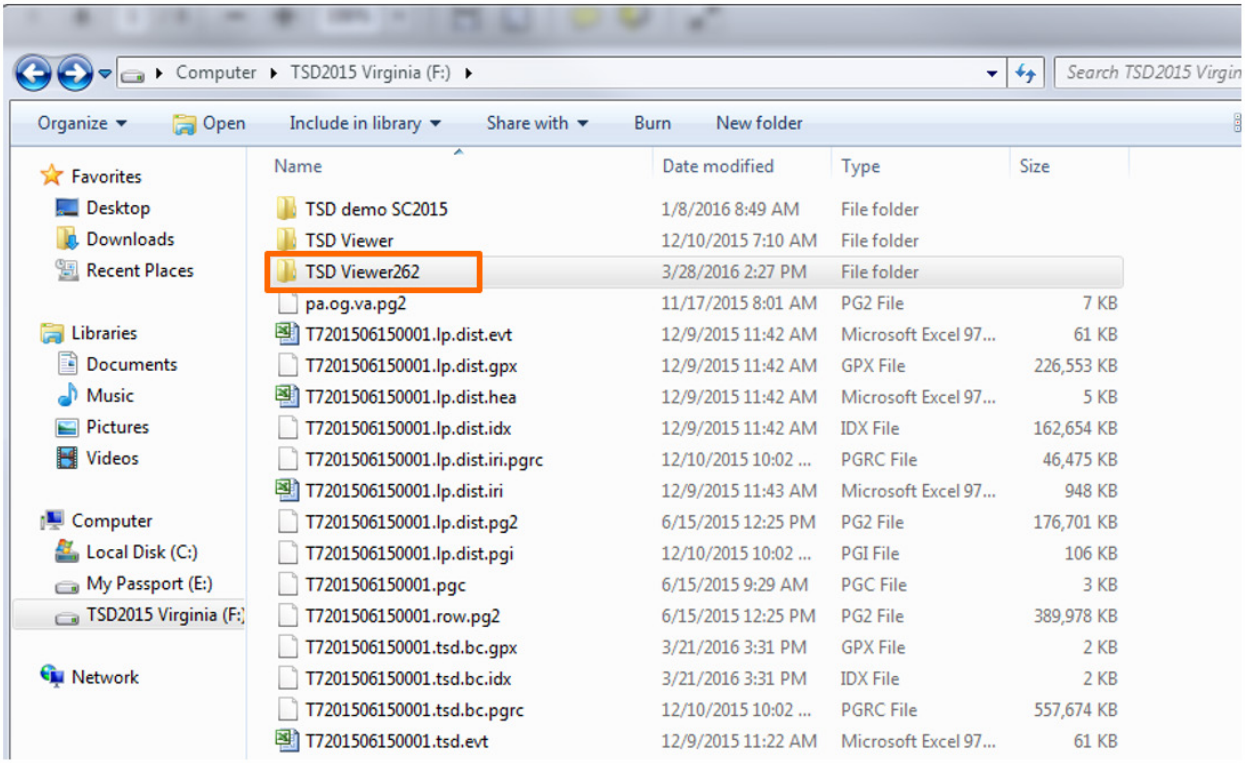

Figure 38. TSD Viewer262 folder.

In the TSD Viewer262 folder, select the application pghw as shown in Figure 39.

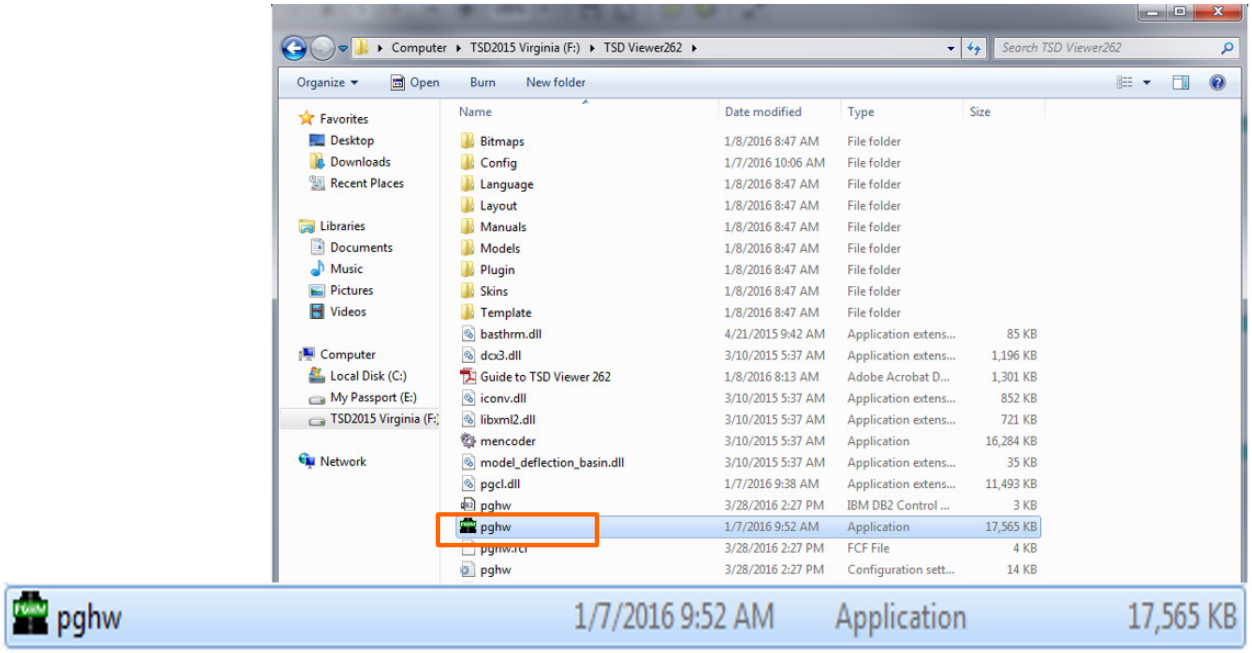

Figure 39. TSD profilograph application pghw.

The profilograph window will open as shown in Figure 40. Before opening a file, the user can set the preferences.

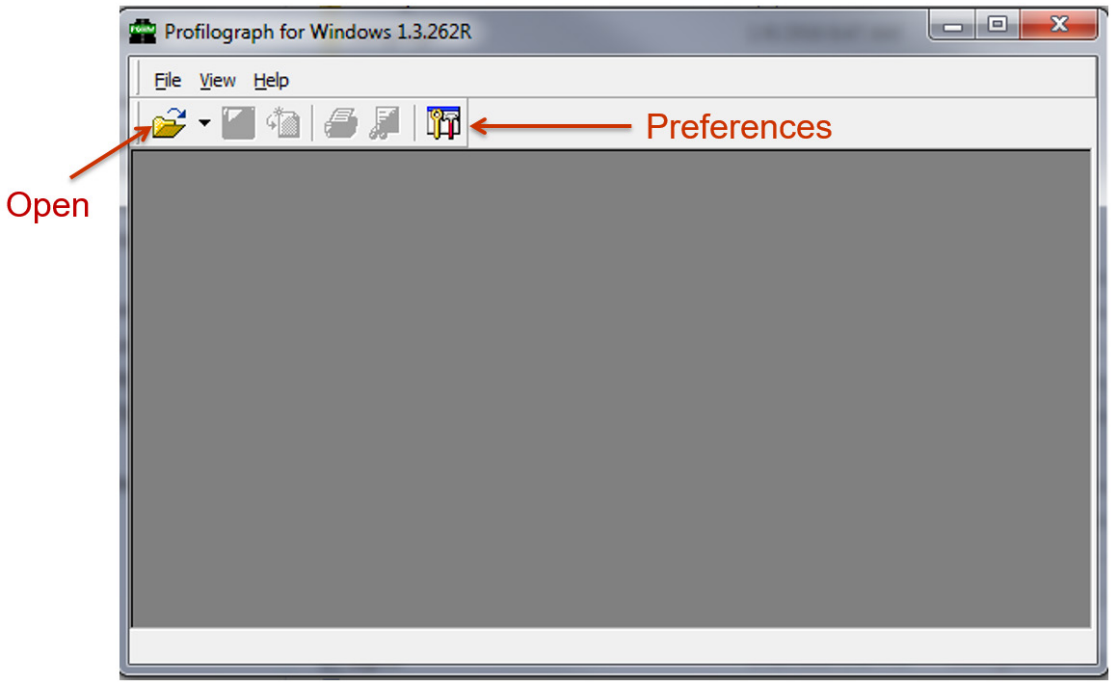

Figure 40. Main window of TSD profilograph.

The preferences can be used to select the units used to display the data as shown in Figure 41.

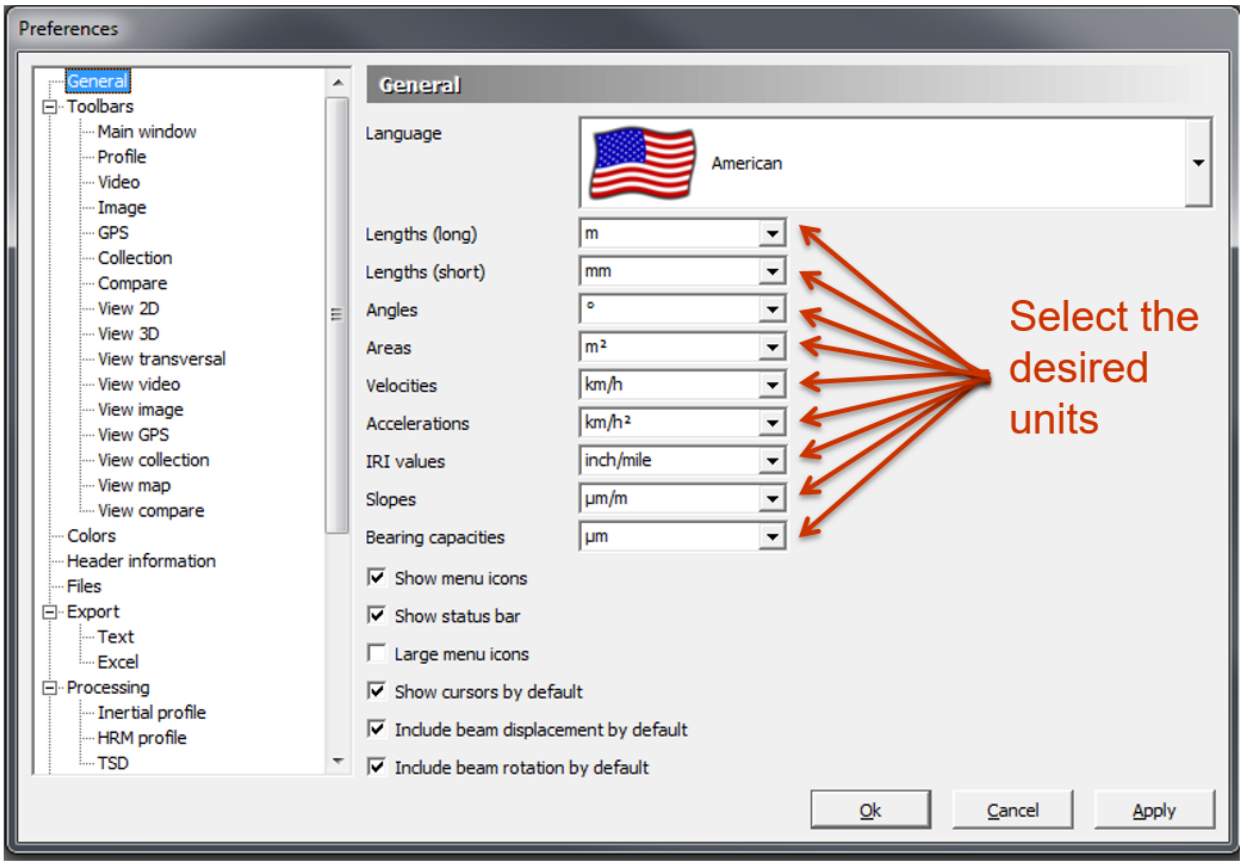

Figure 41. Window to adjust preferences.

In the preferences, click Files from the list in the left pane and select the appropriate path for the profilograph viewer (this will usually be the USB drive) as shown in Figure 42.

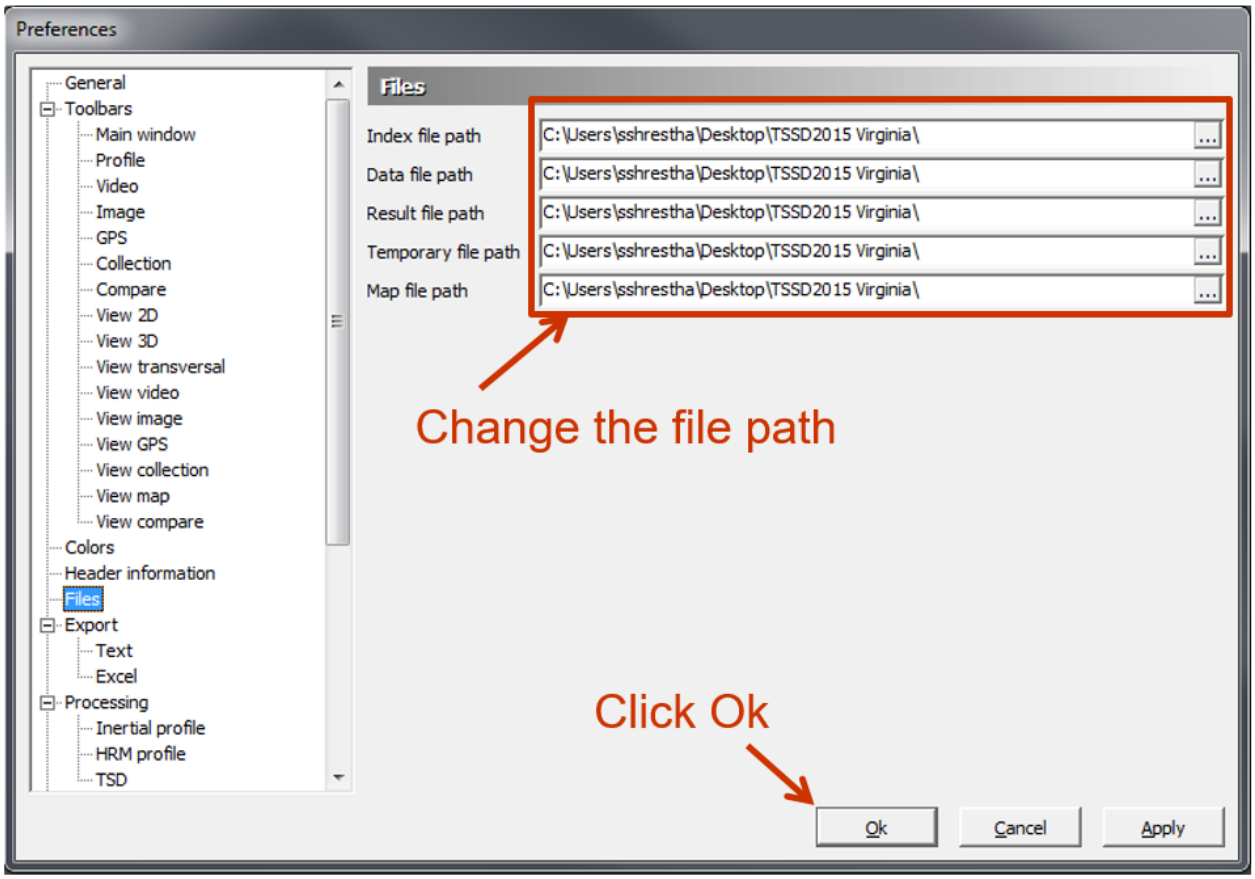

Figure 42. Selecting the file path.

Once the correct paths have been selected, click the Open icon as shown in Figure 43.

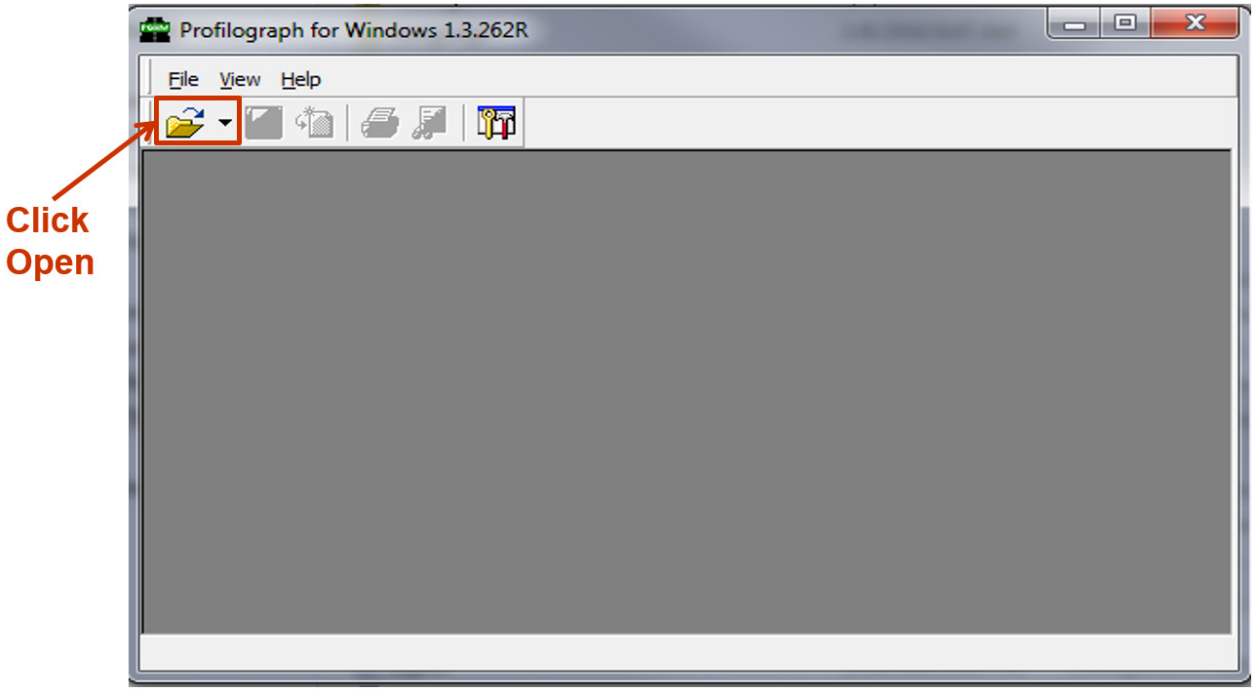

Figure 43. Opening folder.

A window will open. Select a file with the extension ".pgc" as shown in Figure 44. The first time the file is opened, the data are synchronized, which may take more than 30 minutes (depending on the file size). If the file has already been processed, an error message shown in Figure 45 will pop up; just click Ok.

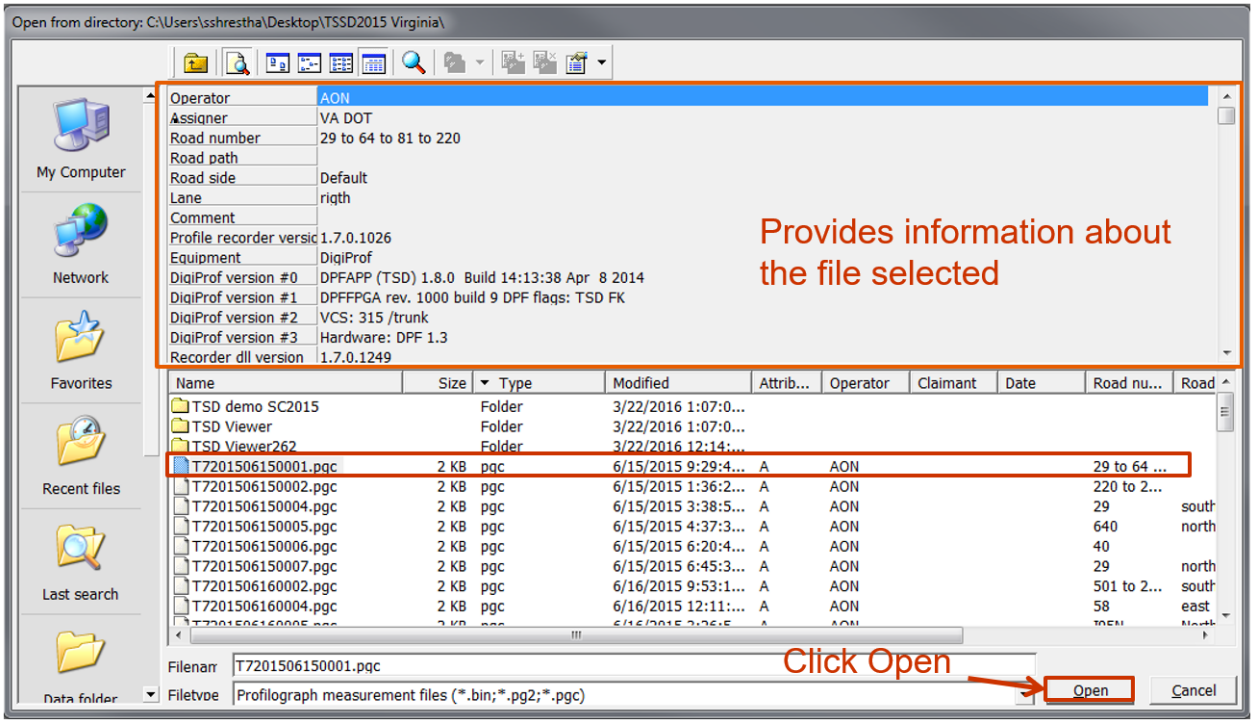

Figure 44. Browse window to select file.

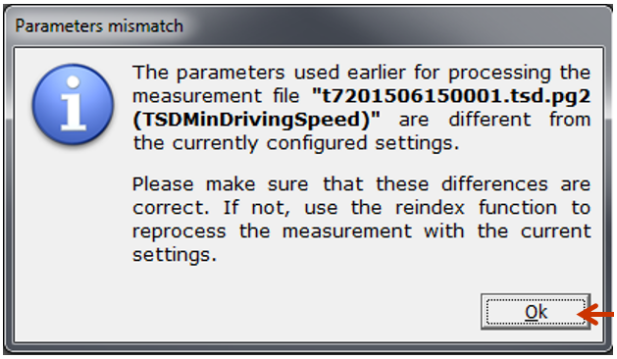

Figure 45. Message showing that the selected file had already been processed.

The software will combine all the results into one window as shown in Figure 46.

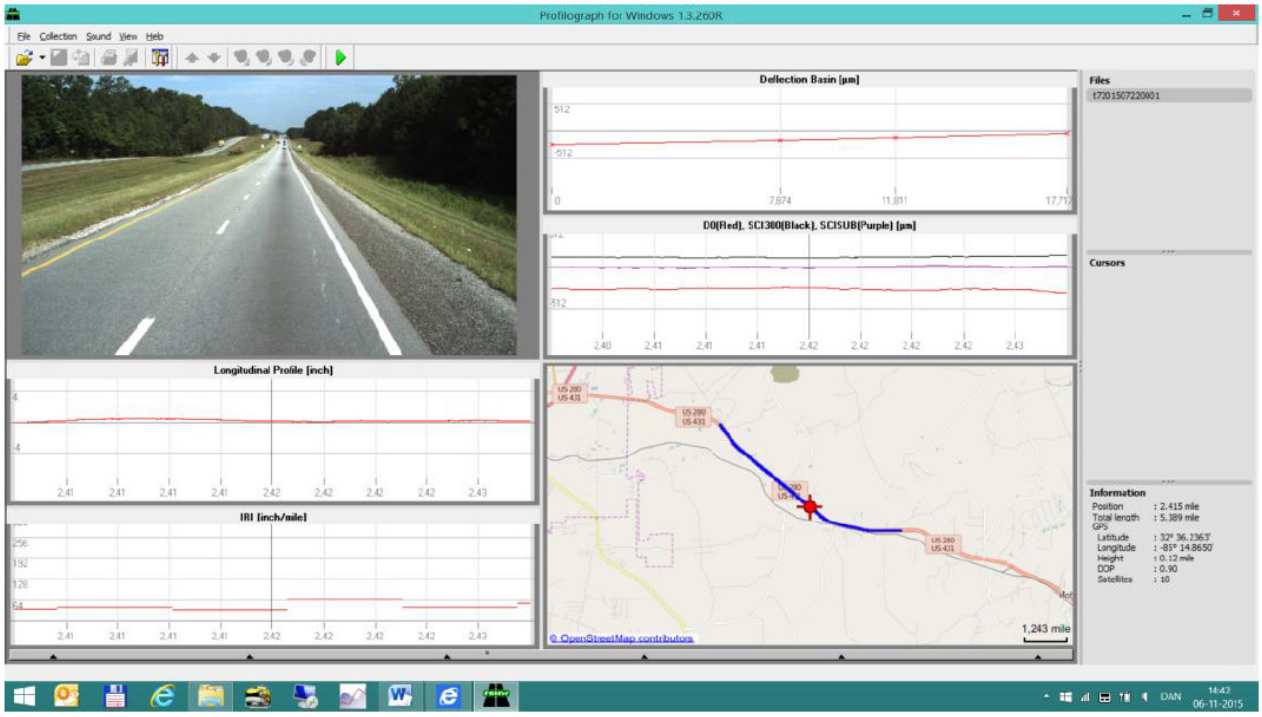

Figure 46. Display windows after file is synchronized.

Different commands can be accessed through the Collection menu. Click on the command bar as shown in Figure 47. A menu opens up with the options, Speed, Events, Displacement, Jump, and Make Video. (Note: Currently, Make Video is not available, and clicking it will cause the program to crash.)

Play: The Play button is also represented by a green button in the Command bar. It can be used to play and pause the data in the main window.

Speed: The Speed menu represents the relative speed of playback and can be used to control the speed of the data shown in the main window. As shown in Figure 47, the speed can be set to Half, Normal, and Double.

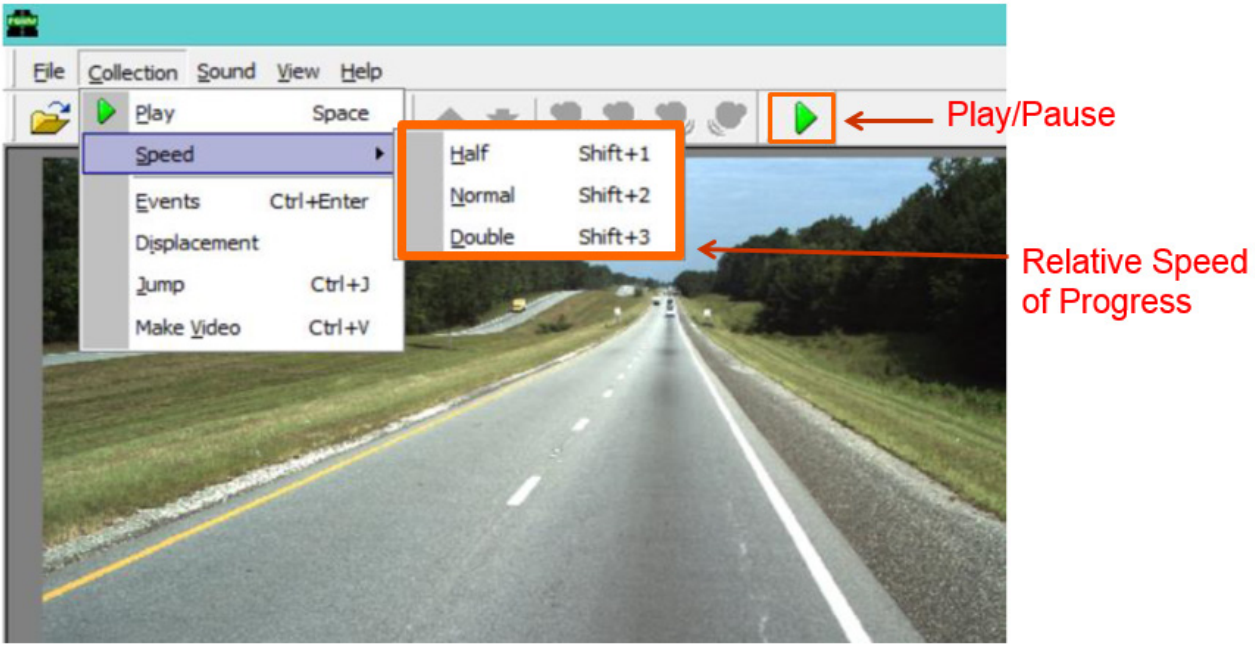

Figure 47. Play button and play speed adjustment option.

Events: The Events option displays the event input made by the operator during measurement recording. You can see the same information if you place the cursor on one of the tiny black triangles in the grey bar at the bottom of the window, as shown in Figure 48. Clicking Events in the menu will cause a window to pop up that shows a list of all the events and the distance at which each is located (Figure 49).

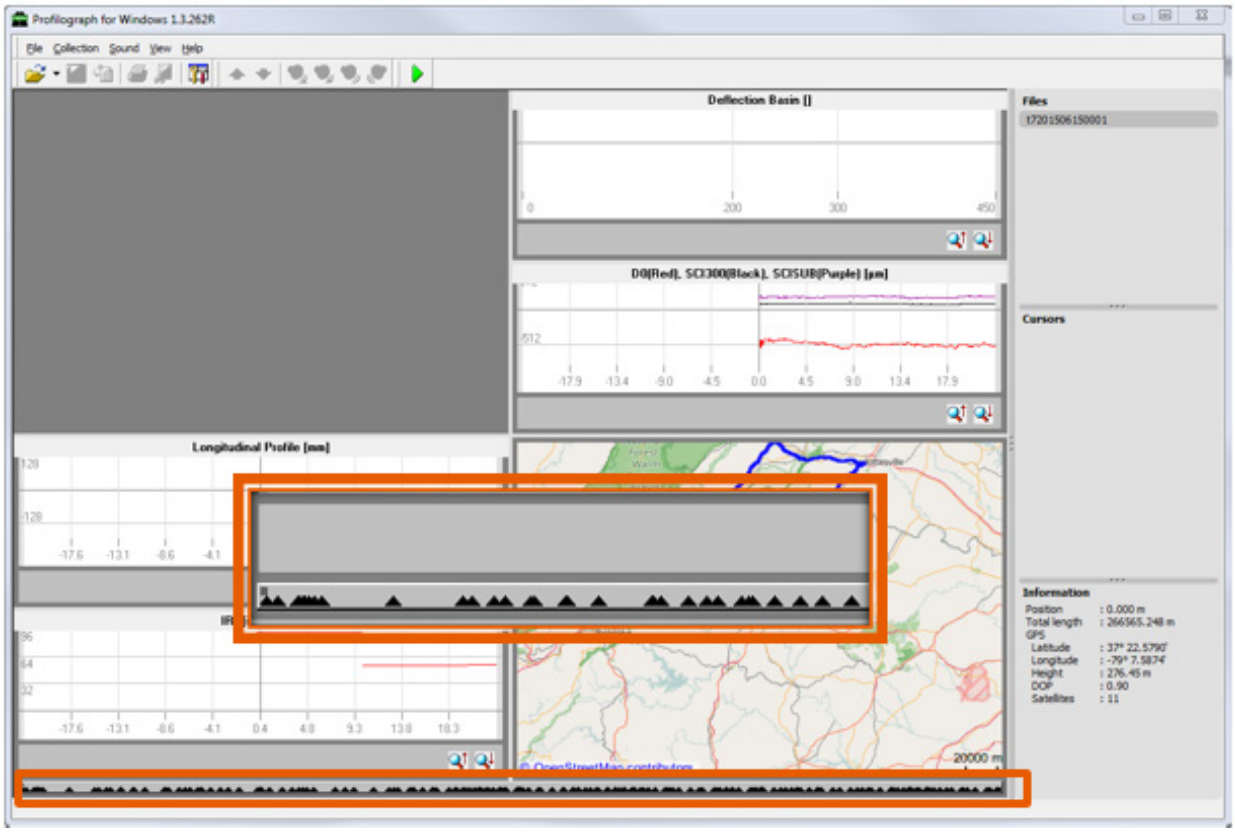

Figure 48. Event bar.

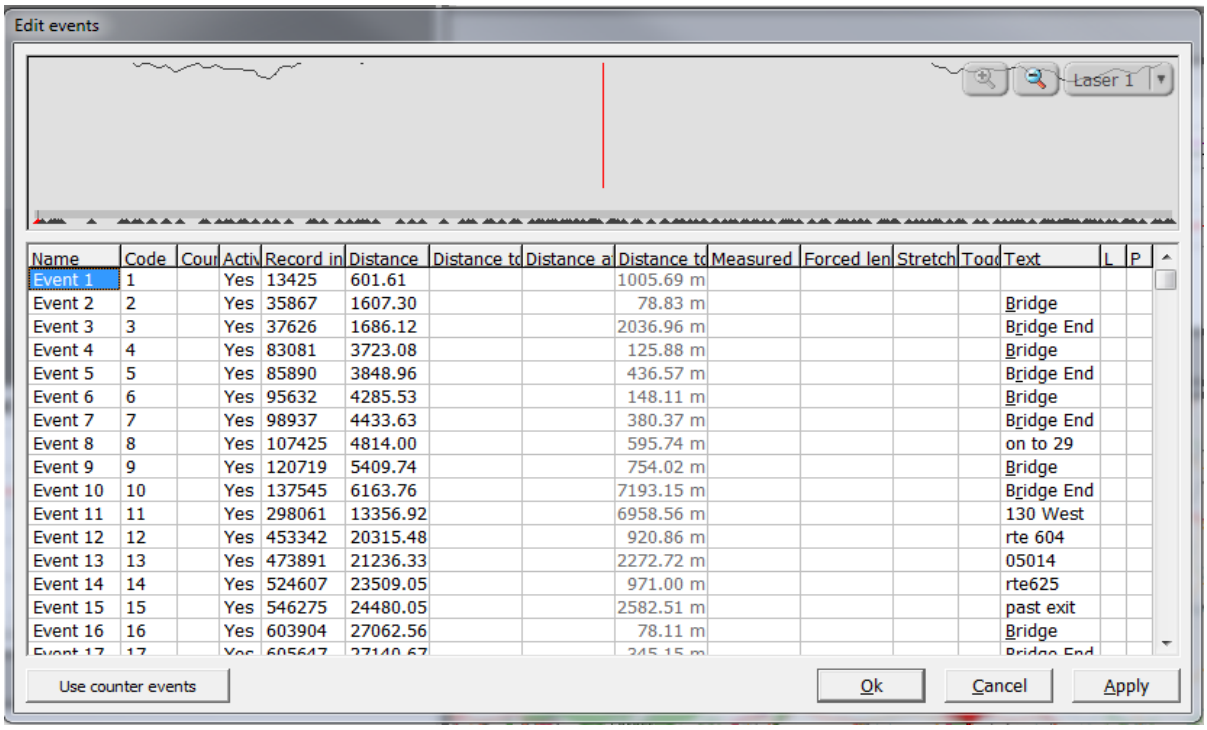

Figure 49. List of events.

Displacement: Click Displacement to adjust the distance between the image, profile, and TSD data. A window will pop up where you can change the distance for the main image, TSD profile, and the longitudinal profile, as shown in Figure 51.

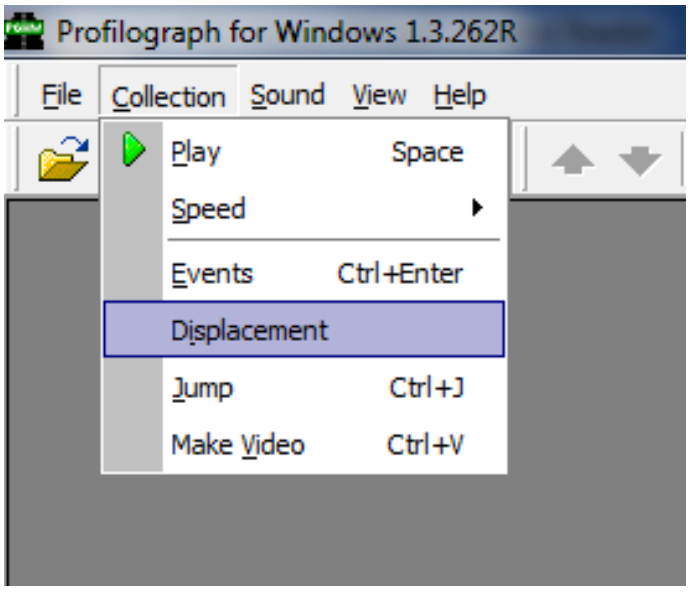

Figure 50. Displacement adjustment between collected data.

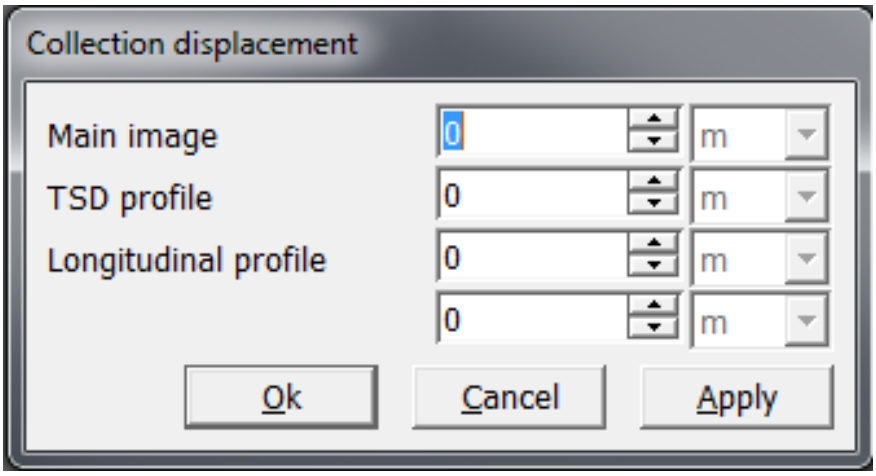

Figure 51. Displacement adjustment between collected data.

Jump: To jump to a chainage with respect to a relative position, click the Collection menu and then click Jump (Figure 52). A window appears (Figure 53) where you can set up the position you want. Click the box, enter the position you want, and click Ok. If you want to change the relative position, click the arrow pointing downward, as shown in Figure 54, and choose the relation you need.

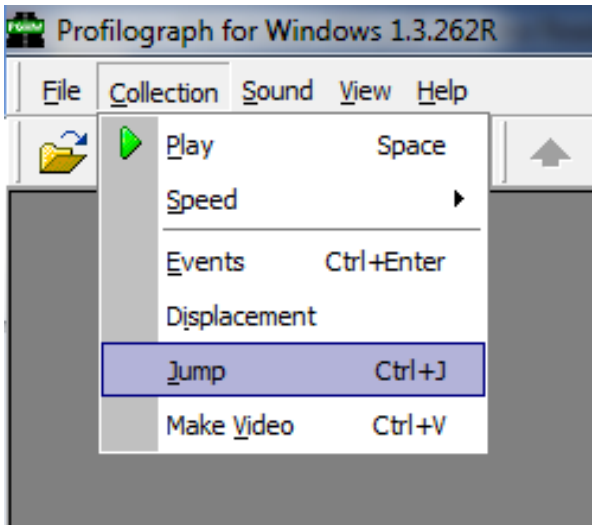

Figure 52. Option to jump to different parts of the data collection.

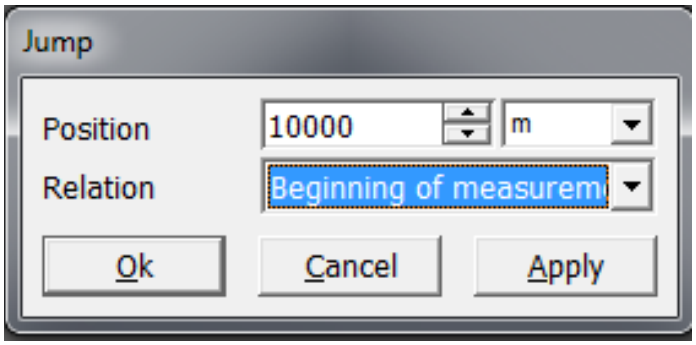

Figure 53. Jump from beginning of measurements.

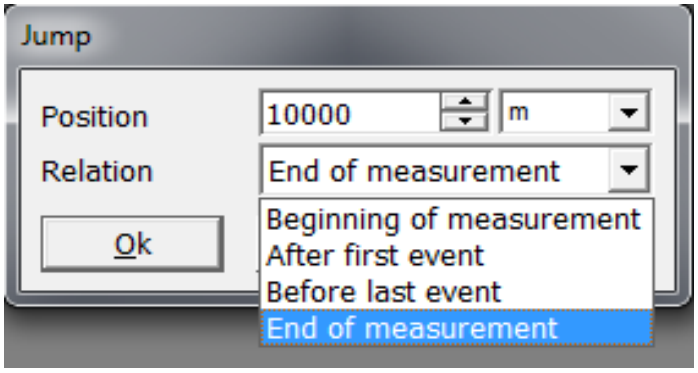

Figure 54. Jump from end of measurements.

Make Video (Warning–Do Not Click): This command is not available at the moment. Clicking this command will crash the program.

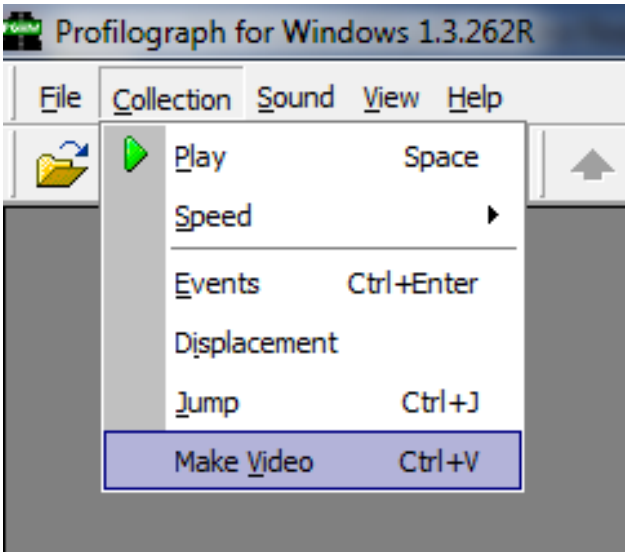

Figure 55. Make video option (not active).